Fractional PID Consensus Control Protocols for Second-Order Multiagent Systems*

David Yaylali[†] and Eric Butcher[‡]
University of Arizona, Tucson, AZ 85721, USA

Arman Dabiri[§]
Eastern Michigan University, Ypsilanti, MI 48197, USA

We outline the formalism and investigate the efficacy of fractional PID$^\alpha$ consensus control for second-order multiagent systems in which the derivative feedback is allowed to take non-integer order. Using algebraic graph theory to characterize the communication topology, a pseudostate-space formalism is developed in terms of the graph Laplacian matrix and used to prove that, given certain conditions on the system's eigenvalues, consensus is guaranteed to be reached asymptotically. We show that these eigenvalue conditions correspond to particular regions of $\{k_P, k_I, k_D, \alpha_D\}$ parameter space and demonstrate this numerically as well as analytically for the special case of a complete graph. Finally, we show that fractional-order controllers outperform standard integer-order controllers in terms of common performance specifications for a selection of benchmark 5-agent systems.

I. Introduction

The study of automated multiagent systems is becoming increasingly ubiquitous in a variety of fields. An important subfield of this discipline is the automated control of multivehicle systems; wide-ranging application areas include spacecraft formation flying, cooperative search and rescue, large aperature space telescopes, rendezvous, and attitude alignment (see [1–3] and references therein). The appearance of illuminated drone-formation displays at recent events such as the 2018 Winter Olympics suggests that applications of this technology are beginning to flourish.

Central to many of these applications is the utilization of consensus control protocols for double-integrator systems [4, 5] due to the second-order dynamics inherent in Newton's laws. Consensus in this context is the convergence of all vehicles to some common values in position and velocity, or to the *convex hull* defined by reference values in the case of a leader/follower consensus scenario [6]. Consensus protocols rely on information sharing between the agents making up the system. A powerful approach to this problem utilizes algebraic graph theory to capture and characterize the communication topology and information flow between the agents [2].

For consensus control of double-integrator systems, the feedback control typically contains information on the relative positions and velocities of the agents. The control protocol for one agent can thus depend on the distance and relative velocity to all other agents with which it shares information. A common consensus control protocol involves feedback of the errors in the position differences between agents which share information as well as the relative velocities to build control protocols which drive these differences and errors to zero. These two components essentially make up a proportional-derivative (PD) consensus controller, whose performance can be tuned based on the relative weight (specified by gains) of the position and velocity feedback terms in the control protocol. Framing the standard consensus control protocol as a PD controller immediately suggests the possibility of adding a third term to the controller proportional to the integral of the position differences. One well-known benefit of adding such a term to a PD-type controller is the reduction in steady-state errors arising from unmodeled dynamics or disturbances. In addition, the tunable gain associated with the integral term in these proportional-integral-derivative (PID) consensus controllers

*This research was supported by the Dynamics, Control, and Systems Diagnostics Program of the National Science Foundation under Grant CMMI-1561836.

[†]MS Student, Department of Aerospace and Mechanical Engineering, University of Arizona, AIAA Member.
[‡]Professor, Department of Aerospace and Mechanical Engineering, University of Arizona, AIAA Member.
[§]Assistant Professor, School of Engineering Technology, Eastern Michigan University.

allows more freedom in shaping the response of the controller, and thus the speed and manner in which the agents in the system reach consensus.

This ability to tune performance is perhaps the main reason why PID controllers are so widely used in industrial and GNC applications. Despite this freedom, certain performance specifications resulting from PID control are inherently coupled. For instance, one may want to design the controller to minimize both rise time and overshoot, but this could lead to unacceptably large control inputs. From a degree-of-freedom standpoint, in best-case scenarios one can only independently tune three performance criteria by adjusting these three gains independently. We therefore may be motivated to add a degree of freedom to our control protocol, so that we have more freedom in shaping the response. One innovative way of introducing extra degrees of freedom is by adjusting the action of the derivatives and integrals themselves.

Fractional calculus offers ways to assign meaning to non-integer powers of the differentiation and integration operators [7]. Although presently a rather obscure subject, a vision of fractional calculus was in fact evident to the pioneers of the ordinary, integer-order calculus including Leibniz, and some years later Euler. It was not until the latter half of the 20^{th} century, however, when applications of these formal concepts began to appear. Natural and mechanical systems which are more accurately or efficiently modeled by fractional-order differential equations of motion include lossy transmission lines, heat diffusion into semi-infinite solids, damping of a plate suspended in viscous liquid, fluid flow and rheology, and certain electric circuits (see [8–10] for reviews). Bagley and Calico found that viscoelastically damped structures exhibit behavior which is effectively described by fractional differential equations [11], and developed a fractional state-space formalism which simplified the description of such systems and suggested the use of fractional feedback control.

Fractional control strategies were developed in the late 20th century, led in large part by investigations by Oustaloup [12] and Podlubney [13]. In some cases, one seeks to control a system whose equations of motion involve non-integer-order derivatives or integrals; in others, one may seek to design controllers for integer-order systems using fractional derivatives or integrals of the system's state. In both cases, the closed-loop equations of motion for the system become fractional in nature. Investigations by Matignon [14], among others, led to important contributions in the understanding of stability of such systems. One of Podlubney's larger contributions was, as alluded to above, the generalization of PID controllers to fractional order $\text{PI}^{\mu}\text{D}^{\nu}$ controllers [13], with integral and derivative control of order μ and ν, respectively, where $0 < \mu, \nu \leq 1$ and integer-order PID control is obtained with $\mu, \nu = 1$. These fractional $\text{PI}^{\mu}\text{D}^{\nu}$ controllers can outperform their integer-order counterparts (see, *e.g.*, [15]).

A fractional $\text{PI}^{\mu}\text{D}^{\nu}$ controller was used for spacecraft attitude control in [16], where it was demonstrated that the fractional controller outperformed standard PID control in terms of certain performance criteria such as the simultaneous optimization of both settling time and overshoot. Consensus control for double-integrator systems using integer-order PD controllers was considered in [5], while proportional-type consensus protocols for fractional-order systems was considered in [17]. Feedback of the integral of an error signal was incorporated into consensus controllers in [18], allowing a multiagent system to achieve consensus in the presence of persistent disturbances. To the best of our knowledge, however, utilization of integer- or fractional-order PID consensus controllers for double-integrator systems has not yet been considered. Therefore, in this paper we explore the problem of fractional PID^{ν} consensus control of a second-order multiagent system with a single spatial coordinate, in which the order of the derivative term in the feedback controller is allowed to take on non-integer values.

In Section II we present a brief review of consensus control for multiagent systems, and introduce the necessary fractional calculus needed for this work. Integer-order PID consensus controllers are also introduced, and in the case of double-integrator systems the conditions on the controller gains for closed-loop stability are derived. In Section III we introduce the fractional PID consensus controller, and in Section IV we prove the stability of a double-integrator multiagent system under this protocol. We present numerical simulations of some benchmark systems in Section V in order to illustrate the advantages of fractional PID^{ν} consensus controllers over standard (integer-order) PD and PID control protocols. We conclude in Section VI.

II. Background Formalism and PID Consensus Control

In this section we review the formalism of multiagent systems and introduce integer-order PID consensus control protocols. We will then introduce fractional calculus, which will be used in Section III to construct a more general fractional-order PID$^\nu$ consensus controller.

A. Integer-Order PID Consensus Protocols

Let us consider a system of N free point-mass agents in one spacial dimension, each of which evolve under applied control forces according to Newton's second law, $F_i = m_i \ddot{r}_i$, with initial conditions $r_i(0) = r_{i0}$ and $\dot{r}_i(0) = v_{i0}$. The following results easily generalize to $D > 1$ spacial dimensions. Defining $u_i = F_i/m_i$ as the control input and $z_i = [r_i \;\; \dot{r}_i]^T$ as the state of agent i, this system is represented by the *double-integrator* state equations

$$\dot{z}_i = \begin{bmatrix} 0 & 1 \\ 0 & 0 \end{bmatrix} z_i + \begin{bmatrix} 0 \\ 1 \end{bmatrix} u_i, \quad z_i(0) = [r_{i0} \;\; v_{i0}]^T, \quad i = 1, 2, \ldots, N. \tag{1}$$

We assume that the agents can communicate with each other according to a prescribed constant communication network, so that the control signal for agent i can depend on its own state as well as those of its neighbors it is in communication with. The communication flow between the agents is encoded in the *communication graph* $\mathcal{G}$ of the system. The formalism used to describe the communication flow is known as algebraic graph theory (see [2, 3] for reviews). This formalism will be crucial for an efficient discussion of consensus control protocols.

Let each agent (identified by the index $i \in \mathcal{N} = \{1, 2, \ldots, N\}$) be associated with a system *node* (or, *vertex*) ν_i (Greek letter "*nu*," not to be confused with velocity v). The set of all vertices is denoted by $\mathcal{V}$. If agent ν_i provides information to agent ν_j, we say that there exists an *edge* (ν_i, ν_j). The set of all edges in the communication topology is denoted by $\mathcal{E}$, and we have $\mathcal{E} \subset \mathcal{V} \times \mathcal{V}$. We note that by definition, $(\nu_i, \nu_i) \notin \mathcal{E}$, so there are no "self-loops". Pictorially, we can represent each node ν_i as a point and the edge (ν_i, ν_j) as an arrow from ν_i to ν_j, as illustrated for a specific 6-agent system in Fig. 1. Thus, the communication topology for a given system is completely characterized by the communication graph $\mathcal{G} = (\mathcal{V}, \mathcal{E})$. If for any edge $(\nu_i, \nu_j) \in \mathcal{E}$ we also have $(\nu_j, \nu_i) \in \mathcal{E}$, the communication graph is said to be *bidirectional*. If edges exist such that one node can communicate to all other nodes in the system, the graph is said to have a *spanning tree*, and the graph is said to be *connected*; the first node along this communication path is known as the *root* node. Additionally, if every possible edge exists (*i.e.*, $(\nu_i, \nu_j) \neq 0, \; \forall i \neq j$), then the graph is said to be *complete* and the communication topology is *fully connected*; in this case, all nodes in the system are root nodes.

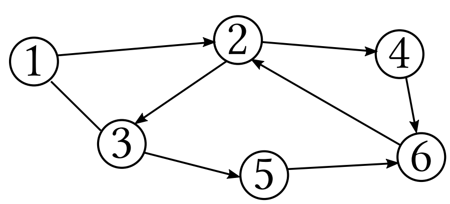

Fig. 1 Pictoral representation of a directed communication graph for a 6-agent system. This graph contains a spanning tree: $1 \to 3 \to 5 \to 6 \to 2 \to 4$. **Note that the communication between node 1 and 3 is undirected.**

The communication topology is encoded in the *graph Laplacian matrix*, constructed as follows. Let us associate with each edge $(\nu_j, \nu_i) \in \mathcal{E}$ a weight $a_{ij} > 0$. If agent ν_j does not communicate with agent ν_i, then $a_{ij} = 0$. We define the $N \times N$ *adjacency matrix* $\mathcal{A}$ by the elements a_{ij}. By definition, the diagonal elements have zero weight, *i.e.*, $a_{ii} = 0$. If $a_{ij} = a_{ji}$ for all edges in the communication topology, the graph is said to be *undirected* and $\mathcal{A}$ is symmetric. We also define the weighted *in-degree* of a node ν_i as the i^{th} row-sum of $\mathcal{A}$, $d_i = \sum_{j=1}^{N} a_{ij}$; the *in-degree matrix* is then $\mathcal{D} \equiv \text{diag}(d_1, d_2, \ldots, d_N)$. The graph Laplacian matrix L is now constructed from the difference of the in-degree and adjacency matrices, $L = \mathcal{D} - \mathcal{A}$. Note that the row sums of L are identically zero, $\sum_{j=1}^{N} L_{ij} = 0$. From this fact it is clear that rank $L \leq N - 1$, and L has at least 1 zero-eigenvalue. It can be shown that graphs which contain at least one spanning tree have rank $L = N - 1$ and exactly 1 zero-eigenvalue, with all other eigenvalues in the right-half complex plane [2].

Cooperative control laws for the multiagent system Eq.(1) can now be formulated in the language of algebraic graph theory introduced above. The standard second-order consensus control protocol [4] takes the form of a PD-type controller. We now introduce integral control to build a PID-type consensus control protocol, which we write as

$$\begin{aligned} u_i &= \sum_{j=1}^{N} a_{ij} \left(k_I(\xi_j - \xi_i) + k_P(r_j - r_i) + k_D(\dot{r}_j - \dot{r}_i) \right) \\ &= \sum_{j=1}^{N} a_{ij} \left(k_I(\xi_j - \xi_i) + k_P \tfrac{d}{dt}(\xi_j - \xi_i) + k_D \tfrac{d^2}{dt^2}(\xi_j - \xi_i) \right) \end{aligned} \qquad i = 1, 2, \ldots, N \tag{2}$$

where in the second line we have written the protocol entirely in terms of the position integral $\xi_i = \int_0^t r_i(\tau) d\tau$, and where k_P, k_I, and k_D are the proportional, integral, and derivative gains, respectively. Let us redefine z_i as the augmented state for agent i including the integral state, *i.e.*, $z_i = [\xi_i \;\; r_i \;\; \dot{r}_i]^T$, and define the *local* state-vector for the entire system to be $\bar{z} = [z_1^T \;\; z_2^T \;\; \cdots \;\; z_N^T]^T$. The closed-loop dynamics of the entire system under protocol Eq. (2) can be written concisely as

$$\dot{\bar{z}} = \bar{A}_c \bar{z} = [I_N \otimes A_3 - L \otimes B_3 K_3] \bar{z} \tag{3}$$

where $\bar{A}_c$ is the closed-loop system matrix (in the local representation), I_N is the N dimensional identity matrix, and

$$A_3 = \begin{bmatrix} 0 & 1 & 0 \\ 0 & 0 & 1 \\ 0 & 0 & 0 \end{bmatrix}, \quad B_3 = \begin{bmatrix} 0 \\ 0 \\ 1 \end{bmatrix}, \quad K_3 = \begin{bmatrix} k_I & k_P & k_D \end{bmatrix}.$$

We can also represent the closed-loop system in terms of the *global* state vector, defined as $\boldsymbol{z} = [\boldsymbol{\xi}^T \;\; \boldsymbol{r}^T \;\; \dot{\boldsymbol{r}}^T]^T$, with $\boldsymbol{\xi} = [\xi_1 \;\; \xi_2 \;\; \cdots \;\; \xi_N]^T$, and $\boldsymbol{r}$ and $\dot{\boldsymbol{r}}$ defined similarly. In terms of the global state vector, the closed-loop state equation can be written as

$$\dot{\boldsymbol{z}} = A_c \boldsymbol{z} = [A_3 \otimes I_N - B_3 K_3 \otimes L] \boldsymbol{z} \tag{4}$$

with the closed-loop system matrix taking the explicit form

$$A_c = \begin{bmatrix} \mathbf{0} & I_N & \mathbf{0} \\ \mathbf{0} & \mathbf{0} & I_N \\ -k_I L & -k_P L & -k_D L \end{bmatrix}. \tag{5}$$

Note that the closed-loop dynamics expressed in Eqs. (3) and (4) are valid for general linear second-order dynamics (as encoded by a general linear system matrix A), while the block-matrix form in Eq. (5) only applies to double-integrator systems.

Eigen-analysis of the closed-loop system and stability

Consider the state equation corresponding to the closed-loop PID consensus system in the local representation, Eq. (3). The conditions for asymptotic stability of the consensus subspace $r_i = r_j$, $v_i = v_j$, $\forall i, j \in \mathcal{N}$, is obtained by analysis of the eigenvalue spectrum of the closed-loop linear matrix in Eq. (3), which is equivalent [2] to the combined spectrums of

$$A_3 - \mu_i B_3 K_3, \quad i = 1, 2, \ldots, N, \tag{6}$$

where μ_i are the eigenvalues of L. That is,

$$\text{spec}\{I_N \otimes A_3 - L \otimes B_3 K_3\} = \text{spec}\{\text{diag}\{A_3 - \mu_1 B_3 K_3,\; A_3 - \mu_2 B_3 K_3,\; \ldots,\; A_3 - \mu_N B_3 K_3\}\}. \tag{7}$$

The eigenvalues λ_i, $i = 1, \ldots, 3N$, of the closed-loop system are thus easily found from the characteristic equation

$$0 = \prod_{i=1}^{N} \det(\lambda I_3 - (A_3 - \mu_i B_3 K_3)) = \lambda^3 \prod_{i=2}^{N} \det(\lambda I_3 - (A_3 - \mu_i B_3 K_3)). \tag{8}$$

(The second equality in Eq. (8) follows from the fact that the Laplacian matrix always has at least one zero eigenvalue, $\mu_1 = 0$.) We therefore find $3N$ eigenvalues for the closed-loop system matrix $\bar{A}_c$; The first three eigenvalues correspond to the zero-eigenvalue μ_1 of L,

$$\lambda_1 = \lambda_2 = \lambda_3 = 0,$$

and the remaining $3(N-1)$ eigenvalues are determined from the $N-1$ third-order polynomial factors arising from the determinant in Eq. (8).

Let us now assume that the communication graph contains a spanning tree, so that

$$\begin{aligned} \mu_1 &= 0 \\ \operatorname{Re}\mu_i &> 0, \quad i = 2, 3, \ldots, N \end{aligned} \tag{9}$$

The nonzero eigenvalues of the closed-loop system are therefore given by the roots of the $N-1$ separate polynomials

$$\det(\lambda I_3 - (A_3 - \mu_i B_3 K_3)) = \lambda^3 + \mu_i k_D \lambda^2 + \mu_i k_P \lambda + \mu_i k_I$$

for $i = 2, 3, \ldots, N$. Replacing $\mu_i = a_i + ib_i$, $a_i > 0$, for a general connected communication topology, the nonzero eigenvalues of the closed-loop system matrix are the solutions to

$$\lambda^3 + (a_i + ib_i)k_D\lambda^2 + (a_i + ib_i)k_P\lambda + (a_i + ib_i)k_I = 0. \tag{10}$$

That is, the closed-loop system will have three zero-eigenvalues (corresponding to $\mu_1 = 0$) in addition to $N-1$ triplets of (potentially nonzero) eigenvalues found from Eq. (10).

Since Eq. (3) is an LTI consensus system, the system will asymptotically reach consensus if all $3(N-1)$ eigenvalues $\lambda_4, \ldots, \lambda_{3N}$ have negative real-part.* Whether or not this condition is met depends on both the communication topology (through the eigenvalues μ_i) and the gain selections $\{k_P, k_I, k_D\}$. For a given communication topology, we can find the stable regions of $\{k_P, k_I, k_D\}$-space by "tracing" the boundary of the λ stability region. Since the nonzero eigenvalues λ_i must be in the left-half complex plane (LHP), the stability boundary in $\{k_P, k_I, k_D\}$-space is found by replacing $\lambda = i\rho$, for arbitrary $\rho \in \mathbb{R}$, in Eq. (10). Setting both real and imaginary parts separately to zero, the arbitrary position ρ along the imaginary axis can be eliminated and we find

$$k_I = \left(a_i + \frac{b_i^2}{a_i}\right) k_D k_P + \left(\frac{b_i}{a_i}\sqrt{a_i + \frac{b_i^2}{a_i}}\right) k_P^{3/2}.$$

This condition corresponds to a hypersurface in $\{k_P, k_I, k_D\}$-space corresponding to the nonzero L eigenvalue μ_i. The volume V_i below this hypersurface corresponds to a stable region of gain space, since gains chosen within this volume will give closed-loop eigenvalues λ in the LHP. Since we require *all* nonzero eigenvalues λ_i to be in the LHP, the stable region of gain space is given by

$$\{k_P, k_I, k_D\} \in V_2 \cap V_3 \cap \cdots \cap V_N.$$

This is equivalent to the explicit requirement

$$k_I < \min_i \left\{ \left(a_i + \frac{b_i^2}{a_i}\right) k_D k_P + \left(\frac{b_i}{a_i}\sqrt{a_i + \frac{b_i^2}{a_i}}\right) k_P^{3/2} \right\}, \quad i = 2, 3, \ldots, N \tag{11}$$

where, again, $a_i = \operatorname{Re}\mu_i$ and $b_i = \operatorname{Im}\mu_i$. In the case of fully connected topologies (complete graphs $\mathcal{K}_N$), the eigenvalues of the graph Laplacian $L(\mathcal{K}_N) = NI_N - \mathbf{1}_{N\times N}$ are given by

$$\mu_i = \begin{cases} 0 & i = 1 \\ N & i = 2, \ldots, N \end{cases} \tag{12}$$

so that the above stability condition reduces to $k_I < N k_P k_D$.

*See [4] for a proof of this in the case of a PD-type control protocol. The proof for the PID-type protocol of Eq.(2) is similar, and will be a special case of the stability proof for fractional PID$^\nu$ consensus control given in Section IV.

B. Fractional Calculus

We briefly review the necessary formulas and relations of fractional calculus which will be used in this work. For formal treatments of the subject, we refer the reader to [7, 9, 19, 20]. For surveys on the subject which are more specific to dynamical systems and control, we refer the reader to [21–23].

The generalization of the differentiation and integration operators to non-integer orders is conceptually expressed as

$$\frac{d^n f(t)}{dt^n} \equiv D^n f(t), \quad n \in \mathbb{N} \quad \longrightarrow \quad D^\alpha f(t), \quad \alpha \in \mathbb{C},\ \mathrm{Re}(\alpha) > 0$$
$$\int \cdots \int f(t) \underbrace{dt \cdots dt}_{n \text{ times}} \equiv D^{-n} f(t), \quad n \in \mathbb{N} \quad \longrightarrow \quad D^{-\nu} f(t), \quad \nu \in \mathbb{C},\ \mathrm{Re}(\nu) > 0.$$

In this work, we will restrict our attention to real-valued orders $\alpha, \nu \in \mathbb{R}$. There are in fact a number of different definitions for the fractional D operators; we will exclusively use the Caputo fractional derivative [20], which is defined in terms of the Riemann-Liouville fractional integral. The (right-sided, definite) Riemann-Liouville (RL) fractional integration operator of order ν is given by

$$_aD_t^{-\nu} f(t) \equiv \frac{1}{\Gamma(\nu)} \int_a^t (t-\tau)^{\nu-1} f(\tau) d\tau, \quad t > a, \ \ \nu > 0 \tag{13}$$

which is well defined if f is piecewise continuous on $(0, \infty)$ and integrable on any finite subinterval of $[0, \infty)$. That is, $_aD_t^{-\nu} f(t)$ is defined for *locally integrable* functions, $f \in L^1_{\mathrm{loc}}[0, t)$. Note that power functions t^p, $p > -1$, satisfy these conditions. The Caputo derivative operator of order α is then given by

$$_aD_t^{\alpha} f(t) \equiv {}_aD_t^{-(n-\alpha)} \left[\frac{d^n f(t)}{dt^n}\right], \quad t > a, \ \ \alpha > 0, \ \ n = \lceil \alpha \rceil \tag{14}$$

where $\lceil \cdot \rceil$ represents the ceiling function. Since this is an RL integral of an integer-order derivative of f, we require that f is differentiable to order n, and that $f^{(n)}(t) \in L^1_{\mathrm{loc}}[0, t)$.

In this work, we will exclusively take the lower terminal of the integral to be zero; we therefore will often suppress the lower indices when this is the case,

$$_0D_t^\alpha \to D^\alpha$$

It should also be mentioned that, since we are considering second-order agents (*i.e.*, agents with *inertia*), it will be understood that all trajectories of the agents are continuous and differentiable, and thus satisfy the modest continuity and differentiability requirements necessary for the validity of the Caputo derivative. In particular, trajectories can be expanded as power series, with the Caputo derivative of a power function explicitly given by

$$D^\alpha t^p = \frac{\Gamma(p+1)}{\Gamma(p-\alpha+1)} t^{p-\alpha}, \quad \alpha \in \mathbb{R}^+, \ p > 0,$$

and in this case the standard *law of exponents* for derivatives holds: $D^\alpha D^\beta t^p = D^{\alpha+\beta} t^p$, $\alpha, \beta \in \mathbb{R}^+$.

In what follows, we will utilize a function that in fractional calculus serves as a generalization of the exponential function. The *Mittag-Leffler* function is defined as

$$E_\alpha(z) \equiv \sum_{k=0}^{\infty} \frac{z^k}{\Gamma(1+\alpha k)}. \tag{15}$$

The Mittag-Leffler (ML) function is the eigenfunction of the fractional derivative operator; that is, it solves the fractional differential equation $D^\alpha x(t) = a x(t)$ given an initial conditon $x(t_0) = x_0$ as

$$x(t) = x_0 E_\alpha(a t^\alpha). \tag{16}$$

Notice from the series definition Eq. (15), $E_1(x) = \exp(x)$. We show in Fig. 2 the solutions Eq. (16) for $a = -1$, $x_0 = 1$, and for various choices of α. When $\alpha = 1$ we have the typical exponential solution to the differential equation

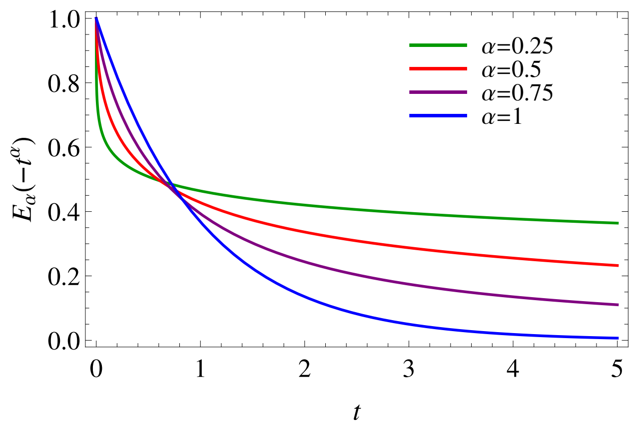

Fig. 2 The behavior of the solutions to $D^\alpha x(t) = -x(t)$, given by $E_\alpha(-t^\alpha)$, for various choices of α. The creeping behavior of the solutions is seen as $\alpha \to 0$.

$Dx(t) = -x(t)$. As α is reduced towards zero, we notice that the solution decays at a slower rate. This "creeping" behavior is a common feature of asymptotically decaying solutions of fractional differential equations. Indeed, in the discussion of stability of fractional systems, it is common to generalize the concept of exponential stability to *Mittag-Leffler (ML) stability* (see, *e.g.*, [24], Definition 4.1).

In the design of consensus controllers as discussed herein, we desire that the our multiagent systems generally reach consensus quickly; This creeping behavior is therefore an undesirable side-effect of using fractional controllers. As we will show numerically, this creeping behavior can be largely mitigated by including integral control in addition to fractional derivative control.

III. General PID Fractional Control for a Consensus System

Let us now consider PID-type fractional control of a system of N agents with a communication topology characterized by the graph Laplacian L. In general, the fractional control protocol for the i^{th} agent is given by

$$u_i = \sum_{j=1}^{N} a_{ij}\Big(\tilde{k}_0 D^{\alpha_0}(\xi_j - \xi_i) + \tilde{k}_1 D^{\alpha_1}(\xi_j - \xi_i) + \cdots + \tilde{k}_{\tilde{m}} D^{\alpha_{\tilde{m}}}(\xi_j - \xi_i)\Big) \qquad i = 1, 2, \ldots, N \tag{17}$$

where $\tilde{k}_i > 0$ and $0 \le \alpha_i < 3,\ \forall i$. Note that we recover the integer-order PID consensus controller, Eq. (2), when $\tilde{m} = 2$, $\alpha_0 = 0$, $\alpha_1 = 1$, and $\alpha_2 = 2$.

A. Equations of Motion in Terms of the Fractional Pseudostate

In what follows we will assume that the fractional derivative orders are rational, $\alpha_i \in \mathbb{Q},\ \forall i$. In this case, the fractional orders α_i in Eq. (17) can be written $\alpha_i = \nu_i/\delta_i$ with $\nu_i, \delta_i \in \mathbb{N}$. Defining δ to be the least common multiple (LCM) of the set $\{\delta_1, \delta_2, \ldots, \delta_{\tilde{m}}\}$, we can write $\alpha_i = n_i/\delta = n_i\alpha$. It is therefore always possible to rewrite Eq. (17) in the form

$$u_i = \sum_{j=1}^{N} a_{ij}\Big(k_0(\xi_j - \xi_i) + k_1 D^{\alpha}(\xi_j - \xi_i) + k_2 D^{2\alpha}(\xi_j - \xi_i) + \cdots + k_m D^{m\alpha}(\xi_j - \xi_i)\Big) \tag{18}$$

where $\alpha = 1/\delta$ is the *fractional order* of the controller. Together with the dynamical equation $D^3\xi_i = u_i$, Eq. (18) describes a *commensurate order* fractional system. We note that the number of non-zero terms does not change when rewriting Eq. (17) as Eq. (18); each term "D^{α_i}" in the former is written as a "$D^{n_i\alpha}$" in the latter. Although in general $m \neq \tilde{m}$, the coefficients k_i will only be non-zero for terms which correspond to the α_i-order terms in Eq. (17).

It is now possible to write the equations of motion for a multiagent system in a form analogous to the state equation Eq. (3). We first consider each agent individually. Since we will utilize integral control (as discussed at the end of Section II.B), let us define the *pseudostate vector* for agent i to be

$$\begin{aligned} \boldsymbol{x}_i &= [\xi_i \;\; D^{\alpha}\xi_i \;\; D^{2\alpha}\xi_i \;\; \cdots \;\; D^{(n-1)\alpha}\xi_i]^T \\ &= [\xi_i \;\; D^{\alpha}\xi_i \;\; D^{2\alpha}\xi_i \;\; \cdots \;\; D^{1-\alpha}\xi_i \qquad r_i \;\; D^{\alpha}r_i \;\; \cdots \;\; D^{1-\alpha}r_i \qquad v_i \;\; D^{\alpha}v_i \;\; \cdots \;\; D^{1-\alpha}v_i]^T. \end{aligned} \tag{19}$$

Note that in the second line we have rewritten the pseudostate in terms of ξ_i, $r_i = \dot{\xi}_i$, and $v_i = \dot{r}_i$ so that all derivatives have fractional order between 0 and 1. The number of pseudostate components n is defined such that the acceleration of the point-mass agent is $\ddot{r}_i = D^3\xi_i = D^{n\alpha}\xi_i$, which implies that $n = 3/\alpha$. Note that since $\alpha = 1/\delta$ and $\delta \in \mathbb{N}$, the number of pseudostate components is guaranteed to be an integer. With this definition, the equations of motion for the i^{th} point-mass agent in terms of the pseudostate $\boldsymbol{x}_i$ is given by the controllable canonical form

$$D^{\alpha}\boldsymbol{x}_i = A_n\boldsymbol{x}_i + B_n u_i, \quad \text{with} \quad A_n = \underbrace{\begin{bmatrix} 0 & 1 & 0 & \cdots & 0 \\ 0 & 0 & 1 & \ddots & \\ \vdots & & \ddots & \ddots & 0 \\ & & & 0 & 1 \\ 0 & \cdots & & & 0 \end{bmatrix}}_{n\times n}, \quad B_n = \begin{bmatrix} 0 \\ 0 \\ \vdots \\ 0 \\ 1 \end{bmatrix}, \tag{20}$$

analogous to the form of the state equation for integer-order PID-controlled systems. The bottom row of this matrix equation gives

$$D^{\alpha}[D^{(n-1)\alpha}\xi_i] = D^{n\alpha}\xi_i = D^3\xi_i = u_i \quad \Rightarrow \quad \ddot{r}_i = u_i,$$

reproducing Newton's second law as desired. Note that this result relies on the fact that the Caputo derivative is being used and that the law of exponents for derivative composition holds (see discussion below Eq. (14); also see [25]).

At this point, one can introduce output equations of the form $\boldsymbol{y}_i = C\boldsymbol{x}_i + Du_i$ representing the accessible (measurable) state components of our system. As a practical matter, in applications one is only able to measure the physical states of the system such as position and velocity, seemingly inhibiting the use of full-pseudostate feedback. Methods of determining the fractional-order pseudostates using fractional observers, however, have been developed and remain an active area of research [26, 27]. Thus, by combining fractional-order observers with the proposed consensus controller, the full pseudostate can be used for feedback.

We note here that defining $1/\alpha = \delta = \text{LCM}[\delta_1, \delta_2, \ldots, \delta_{\tilde{m}}]$ does not always lead to a *minimal* representation. To illustrate, let us consider a single point-mass agent under fractional feedback control of the form

$$u = -D^{3/4}\xi - D^{3/2}\xi$$

(so that this corresponds to a fractional $\mathrm{P}^0\mathrm{I}^{\frac{1}{4}}\mathrm{D}^{\frac{1}{2}}$ controller). Taking the LCM of the denominators of these fractional orders gives $1/\alpha = \delta = 4$, so that our pseudostate comprises $n = 3\delta = 12$ states and our state-equation is of fractional order $\alpha = 1/4$. However, we can equivalently characterize our system by a state equation of fractional order $\bar{\alpha} = 3/4$ using the pseudostate $\boldsymbol{x} = [\xi \;\; D^{\bar{\alpha}}\xi \;\; D^{2\bar{\alpha}}\xi \;\; D^{3\bar{\alpha}}\xi]$. The state-equation is now of dimension 4, with bottom row given by

$$D^{\bar{\alpha}}[D^{3\bar{\alpha}}\xi] = D^{4\bar{\alpha}}\xi = u = -D^{\bar{\alpha}}\xi - D^{2\bar{\alpha}}\xi \quad \Rightarrow \quad D^3\xi = \ddot{r} = -D^{3/4}\xi - D^{3/2}\xi$$

In general, the minimal representation corresponds to a fractional order

$$\bar{\alpha} = \frac{\text{GCD}[3, n_1, n_2, \ldots, n_{\tilde{m}}]}{\text{LCM}[\delta_1, \delta_2, \ldots, \delta_{\tilde{m}}]}$$

where GCD[·] represents the greatest common divisor. Throughout this work, however, we will continue to define the fractional order of the system as $1/\alpha = \text{LCM}[\delta_1, \ldots, \delta_{\tilde{m}}]$, since this gives the minimal representation whenever the controller involves a proportional (*i.e.*. $D^1\xi$) term.

We now define the state vector of the entire N-agent system; as in Section II.A, this can be done in two different ways, defining the *local* and *global* representations. In the local representation, the system state-vector is defined by concatenating the pseudostate vectors for each of the N agents,

$$\bar{\boldsymbol{X}} = \begin{bmatrix} \boldsymbol{x}_1^T & \boldsymbol{x}_2^T & \cdots & \boldsymbol{x}_N^T \end{bmatrix}^T, \tag{21}$$

with $\boldsymbol{x}_i$ defined in Eq. (19). In the global representation, the state-vector of the system is found by concatenating the individual pseudostate components of each agent: defining $\boldsymbol{z} = [\,\xi_1 \;\; \xi_2 \;\cdots\; \xi_N\,]^T$, the system state-vector is constructed as

$$\boldsymbol{X} = \begin{bmatrix} \boldsymbol{z}^T & D^{\alpha}\boldsymbol{z}^T & \cdots & D^{(n-1)\alpha}\boldsymbol{z}^T \end{bmatrix}^T. \tag{22}$$

The dimension of the total state vector in either representation is $(nN \times 1)$.

B. Closed-Loop Equations of Motion

With the dynamics of each agent described by Eq. (20) and the control given by Eq. (18), it is straightforward to show that the closed-loop equations of motion for the system are given by

$$D^{\alpha}\boldsymbol{X} = A_c\boldsymbol{X} = \big(A_n \otimes I_N - B_nK_n \otimes L\big)\boldsymbol{X} \tag{23}$$

in the global representation, and

$$D^{\alpha}\bar{\boldsymbol{X}} = \bar{A}_c\bar{\boldsymbol{X}} = \big(I_N \otimes A_n - L \otimes B_nK_n\big)\bar{\boldsymbol{X}} \tag{24}$$

in the local representation (*c.f.*, Eqs. (4) and (3), respectively). Here, K_n is a row vector containing the gains of each sequential derivative term, as will be illustrated below by example. Since $\boldsymbol{X}$ is related to $\bar{\boldsymbol{X}}$ through permutation, we can easily transform between representations; that is,

$$\boldsymbol{X} = \Lambda\bar{\boldsymbol{X}} \quad \Leftrightarrow \quad \bar{A}_c = \Lambda^T A_c \Lambda$$

where Λ is a (orthogonal) permutation matrix (*i.e.*, $\det\Lambda = \pm 1$ and $\Lambda\Lambda^T = I$). The left equality allows us to construct the explicit form of the permutation matrix as

$$\Lambda = \begin{bmatrix} I_N \otimes P_0 \\ I_N \otimes P_1 \\ \vdots \\ I_N \otimes P_{n-1} \end{bmatrix} \tag{25}$$

where P_j is the $(1 \times n)$ projection operator which projects out the j^{th} pseudostate component, $P_j\boldsymbol{x}_i = D^{j\alpha}\xi_i$.

■ Illustrative Example: 3-agent system under PI$^{1/2}$D$^{1/2}$ control

For this system, the integral control of order $\alpha_I = 1/2$ corresponds to a $D^{1-\alpha_I}(\xi_j - \xi_i) = D^{1/2}(\xi_j - \xi_i)$ term and derivative control of order $\alpha_D = 1/2$ corresponds to a $D^{1+\alpha_D}(\xi_j - \xi_i) = D^{3/2}(\xi_j - \xi_i)$ in the control law. We therefore have derivative orders $\alpha_1 = n_1/\delta_1 = 1/2$, $\alpha_2 = n_2/\delta_2 = 1/1$, and $\alpha_3 = n_3/\delta_3 = 3/2$, and the commensurate order of this system is $\alpha = 1/\text{LCM}[\delta_1, \delta_2, \delta_3] = 1/2$. The control law for the i^{th} agent in commensurate form is thus

$$u_i = \sum_{j=1}^{3} a_{ij}\Big(k_I D^{1/2}(\xi_j - \xi_i) + k_P D^{1}(\xi_j - \xi_i) + k_D D^{3/2}(\xi_j - \xi_i)\Big) \tag{26}$$

$$= \sum_{j=1}^{3} a_{ij}\Big(k_I D^{p\alpha}(\xi_j - \xi_i) + k_P D^{\delta\alpha}(\xi_j - \xi_i) + k_D D^{q\alpha}(\xi_j - \xi_i)\Big) \tag{27}$$

with $p = \alpha_1/\alpha = 1$ and $q = \alpha_3/\alpha = 3$. Since $\delta = 1/\alpha = 2$, there are $n = 3\delta = 6$ pseudostate components per agent. The (1×6) gain matrix K_n has k_I in the $(p+1)$ position, k_P in the $(\delta+1)$ position, k_D in the $(q+1)$ position, and zeros elsewhere:

$$K_n = \begin{bmatrix} 0 & k_I & k_P & k_D & 0 & 0 \end{bmatrix}.$$

The closed-loop pseudostate equation in the global (Eq. (23)) and local (Eq. (24)) representations are given by

$$\text{(Global Rep.):} \qquad D^{1/2}\boldsymbol{X} = \begin{bmatrix} \mathbf{0} & I_3 & \mathbf{0} & \mathbf{0} & \mathbf{0} & \mathbf{0} \\ \mathbf{0} & \mathbf{0} & I_3 & \mathbf{0} & \mathbf{0} & \mathbf{0} \\ \mathbf{0} & \mathbf{0} & \mathbf{0} & I_3 & \mathbf{0} & \mathbf{0} \\ \mathbf{0} & \mathbf{0} & \mathbf{0} & \mathbf{0} & I_3 & \mathbf{0} \\ \mathbf{0} & \mathbf{0} & \mathbf{0} & \mathbf{0} & \mathbf{0} & I_3 \\ \mathbf{0} & -k_I L & -k_P L & -k_D L & \mathbf{0} & \mathbf{0} \end{bmatrix} \boldsymbol{X}$$

$$\text{(Local Rep.):} \qquad D^{1/2}\bar{\boldsymbol{X}} = \begin{bmatrix} L_{11}(A_n - B_n K_n) & -L_{12} B_n K_n & -L_{13} B_n K_n \\ -L_{21} B_n K_n & L_{22}(A_n - B_n K_n) & -L_{23} B_n K_n \\ -L_{31} B_n K_n & -L_{32} B_n K_n & L_{33}(A_n - B_n K_n) \end{bmatrix} \bar{\boldsymbol{X}}$$

The dimension of both of these representations is $nN = 18$. ■

It is important to realize that the dimension nN of the pseudostate equation (Eqs. (23) or (24)) is highly sensitive to the fractional order α, and can become quite large. To illustrate, let us take a specific case of an integer-order PI controller with fractional derivative control. In the incommensurate form of Eq. (17), this corresponds to

$$u_i = \sum_{j=1}^{N} a_{ij} \left(k_I D^0(\xi_j - \xi_i) + k_P D^1(\xi_j - \xi_i) + k_D D^{1+\alpha_D}(\xi_j - \xi_i) \right) \tag{28}$$

If we take $\alpha_D = 0.5$, the (commensurate) fractional order of the system is $\alpha = \frac{1}{2}$ and the number of pseudostates (the dimension of $\boldsymbol{X}$) is $3N/\alpha = 6N$. If we instead take $\alpha_D = 0.51$, then the fractional order of the system is $\alpha = 1/100$ (so that $\alpha_D = 51\alpha$) and the dimension of the pseudostate equation is $300N$. In general, if there are p digits in the mantissa of α_D, then $\dim\boldsymbol{X} \leq 3 \times 10^p \times N$.

It therefore becomes apparent that the pseudostate-space formalism introduced above is ill-suited for certain practical applications such as numerical simulation of general fractional systems or fractional PID tuning. Nevertheless, the pseudostate-space form, which in principle is valid for any rational fractional orders α_i, allows one to efficiently study the stability properties of a (rationally-ordered) fractionally controlled system.

IV. PID$^\alpha$ Control — Closed-Loop Stability

In the remainder of this work, we will restrict our attention to PID$^\alpha$ consensus control protocols of the form given in Eq. (28), and take $0 < \alpha_D < 1$. Using fractional derivative control gives an extra degree of freedom (fractional order α_D) which can be tuned to achieve more optimal system response characteristics. In this section we will prove that, under certain conditions, a multiagent system will asymptotically (in the Mittag-Leffler sense; see discussion after Eq. (16)) reach consensus in position and velocity for any initial conditions.

In what follows we will assume that the communication topology of the system has a spanning tree. In this case the graph Laplacian matrix L has a simple zero-eigenvalue μ_1 and, according to Geršgorin's circle theorem, the remaining $N-1$ eigenvalues are in the right-half plane. We label these eigenvalues according to $|\mu_1| < |\mu_2| \leq \cdots \leq |\mu_N|$.

A. Eigen-Analysis of the PID$^\alpha$ Controlled Closed-Loop System

Consider an N-body multiagent system under control protocol Eq. (28). Assuming $\alpha_D \in \mathbb{Q}$, we can represent this control protocol in commensurate form

$$\begin{aligned} u_i &= \sum_{j=1}^{N} a_{ij} \left(k_I(\xi_j - \xi_i) + k_P(r_j - r_i) + k_D D^{\alpha_D}(r_j - r_i) \right) \\ &= \sum_{j=1}^{N} a_{ij} \left(k_I(\xi_j - \xi_i) + k_P D^{\delta\alpha}(\xi_j - \xi_i) + k_D D^{q\alpha}(\xi_j - \xi_i) \right) \end{aligned} \tag{29}$$

where α is the (commensurate) fractional order of the system, $\delta = 1/\alpha$, $n = 3/\alpha$, and $\{k_I,\ k_P,\ k_D\} \geq 0$. In this case, since the derivative orders of the first and second terms are 0 and 1, the fractional order α is determined purely from α_D. Since this derivative order is rational we can write $\alpha_D = \nu_D/\delta_D$, so that $\alpha = 1/\delta_D$. Also, since we are assuming the fractional order $0 \leq \alpha_D \leq 1$, we have $\delta < q < 2\delta$.

The closed-loop dynamics are given in the local representation by Eq. (24). As in the integer-order case, since

$$\mathrm{spec}\Big\{I_N \otimes A_n - L \otimes B_n K_n\Big\} = \mathrm{spec}\Big\{\mathrm{diag}\big(A_n,\ A_n - \mu_2 B_n K_n, \cdots,\ A_n - \mu_N B_n K_n\big)\Big\},$$

the eigenvalues of the closed-loop system can be found by solving the characteristic equation for the block-diagonal matrix on the right-hand side. This is given by

$$0 = \det(\lambda I_n - A_n) \prod_{i=2}^{N} \det(\lambda I_n - A_n + \mu_i B_n K_n) \tag{30}$$

$$= \lambda^n \prod_{i=2}^{N} \det(\lambda I_n - A_n + \mu_i B_n K_n) \tag{31}$$

We therefore immediately see that the simple zero-eigenvalue of the graph Laplacian corresponds to n zero-eigenvalues of the closed-loop system. The remaining eigenvalues can be found by solving for the roots of the $N-1$ separate n^{th}-order polynomials,

$$0 = \det(\lambda I_n - A_n + \mu_i B_n K_n) = k_I \mu_i + k_P \mu_i \lambda^\delta + k_D \mu_i \lambda^q + \lambda^n \quad i = 2, \ldots, N,$$

each of which provides n additional eigenvalues; for $k_I > 0$, these additional eigenvalues are non-zero. Note that, since A_c and $\bar{A}_c$ are related through a similarity transform, they will share the same eigenvalues.

B. Stability for Fractionally Controlled Systems

We will now prove that, given a PID$^\alpha$-controlled multiagent system whose communication topology contains a spanning tree, consensus is reached asymptotically if all non-zero eigenvalues of the closed-loop system matrix A_c satisfy $|\arg \lambda_i| > \alpha\pi/2$. This condition on the non-zero eigenvalues is an instance of Matignon's theorem [14]. The following proof generalizes the stability proof for standard PD consensus control as given in [4].

Consider the pseudostate equation for this system in the global representation, Eq. (23),

$${}_0D_t^\alpha \boldsymbol{X}(t) = A_c \boldsymbol{X}(t), \tag{32}$$

with $0 < \alpha \leq 1$ and with initial conditions $\boldsymbol{X}(0) \equiv \boldsymbol{X}_0$. Substituting into this equation the power series expansion

$$\boldsymbol{X}(t) = \boldsymbol{X}_0 + \boldsymbol{X}_1 t^\alpha + \boldsymbol{X}_2 t^{2\alpha} + \cdots$$

and equating like powers of t, one find the *pseudo*state transition matrix (pSTM) $\Phi_\alpha(t, 0)$ for this system as [11]

$$\boldsymbol{X}(t) = \Phi_\alpha(t,0)\boldsymbol{X}_0 = \left(I + \frac{A_c t^\alpha}{\Gamma(1+\alpha)} + \frac{A_c^2 t^{2\alpha}}{\Gamma(1+2\alpha)} + \cdots\right)\boldsymbol{X}_0 \tag{33}$$

$$\equiv E_\alpha[A_c t^\alpha]\boldsymbol{X}_0 \tag{34}$$

where we have here defined the *matrix* Mittag-Leffler function $E_\alpha[M]$ (*c.f.*, Eq. (15)). Note that, since the ML function reduces to the exponential function as $\alpha \to 1$, the pSTM stands in direct analogy to the STM for integer order systems, $\Phi(t, 0) = \exp[A_c t]$. Unlike the integer-order STM, however, $\Phi_\alpha(t, t')\Phi_\alpha(t', 0) \neq \Phi_\alpha(t, 0)$ since the ML function does not satisfy the semigroup property $f(x)f(y) = f(x + y)$. This is intimately connected to the fact that fractional derivatives are *non-local*, in that they depend on their initial conditions through the integration window of the RL integral in Eq. (14).

As shown in the previous section, since we have integer-order integral control, A_c has exactly n zero-eigenvalues, where $n = 3/\alpha$. That is,

$$\text{eig}\, A_c : \quad \begin{cases} \lambda_j = 0, & j = 1, \ldots, n \\ \lambda_j \neq 0, & j = n+1, \ldots, nN \end{cases}$$

We first show that the zero-eigenvalues of A_c have geometric multiplicity of 1. Let us define $\boldsymbol{q} = [q_1^T \;\; q_2^T \;\; \cdots \;\; q_n^T]^T$ to be the eigenvector associated with $\lambda = 0$, with $q_i \in \mathbb{R}^N$. From Eq. (23) we can find the explicit form of A_c, so that

$$A_c \boldsymbol{q} = \begin{bmatrix} \mathbf{0} & I_N & \mathbf{0} & \cdots & \mathbf{0} \\ \mathbf{0} & \mathbf{0} & \ddots & & \vdots \\ \vdots & & \cdots & & I_N \\ -k_1 L & -k_2 L & \cdots & & -k_n L \end{bmatrix} \begin{bmatrix} q_1 \\ q_2 \\ \vdots \\ q_n \end{bmatrix} = \begin{bmatrix} \mathbf{0} \\ \mathbf{0} \\ \vdots \\ \mathbf{0} \end{bmatrix}.$$

From the upper rows of this block-matrix equation, we find that $q_i = 0$ for $i = 2, \ldots, n$; from the last row we find that $-Lq_1 = 0$. Since L has a spanning tree, L has exactly one zero-eigenvalue $\mu = 0$. This in turn implies that the geometric multiplicity of $\mu = 0$ is 1, and thus that q_1 is the only eigenvector of L associated with $\mu = 0$. Therefore, there is only a single linearly-independent eigenvector which satisfies $A_c \boldsymbol{q} = \lambda \boldsymbol{q} = 0$, namely

$$\boldsymbol{q} = \begin{bmatrix} q_1^T & \mathbf{0} & \cdots & \mathbf{0} \end{bmatrix}^T.$$

Thus the eigenvalue $\lambda = 0$ of A_c has algebraic multiplicity of n and geometric multiplicity of 1.

We can now find the Jordan decomposition of A_c as

$$A_c = VJW = V \begin{bmatrix} J_0 & \mathbf{0}_{n\times\tilde{n}} \\ \mathbf{0}_{\tilde{n}\times n} & J' \end{bmatrix} W$$

where $\tilde{n} = n(N-1)$, and where J_0 is the n-dimensional Jordan block associated with $\lambda = 0$ (since we proved that $\lambda = 0$ has geometric multiplicity of 1, all zero-eigenvalues of A_c are collected into this single Jordan block). The $\tilde{n} \times \tilde{n}$ sub-matrix J' comprises all Jordan blocks associated with the eigenvalues λ_i for $i = n+1, \ldots, nN$. In general, these eigenvalues can all be unique (*i.e.*, simple), in which case $J' = \text{diag}(\lambda_{n+1}, \lambda_{n+2}, \ldots, \lambda_{nN})$. The matrices V and W facilitating the similarity transformation are

$$V = \begin{bmatrix} v_1 & v_2 & \cdots & v_{nN} \end{bmatrix}, \qquad W = \begin{bmatrix} w_1^T \\ w_2^T \\ \vdots \\ w_{nN}^T \end{bmatrix}$$

where $v_i \in \mathbb{R}^{nN\times 1}$ are the right (generalized) eigenvectors of A_c and $w_i^T \in \mathbb{R}^{1\times nN}$ are the left (generalized) eigenvectors of A_c. Since V and W transform A_c to Jordan normal form, we necessarily have $WV = I_{nN}$. This implies that $w_i^T v_j = \delta_{ij}$ for all $i, j \in \{1, 2, \ldots nN\}$.

The matrix ML function applied to $A_c t^\alpha$ is thus

$$E_\alpha[A_c t^\alpha] = V \begin{bmatrix} E_\alpha[J_0 t^\alpha] & \mathbf{0}_{n\times\tilde{n}} \\ \mathbf{0}_{\tilde{n}\times n} & E_\alpha[J' t^\alpha] \end{bmatrix} W \tag{35}$$

The series definition for $E_\alpha[J_0 t^\alpha]$ is easily computed since the matrix J_0 is nilpotent, *i.e.*, $J_0^m = 0$ for $m \geq n$ (recall that n is the dimension of J_0). Explicitly,

$$E_\alpha[J_0 t^\alpha] = \sum_{k=0}^{n-1} \frac{J_0^k t^{k\alpha}}{\Gamma[1 + k\alpha]} = \begin{bmatrix} \Theta_0 & \Theta_1 & \cdots & \Theta_{n-1} \\ 0 & \Theta_0 & \cdots & \Theta_{n-2} \\ \vdots & \ddots & \ddots & \vdots \\ 0 & \cdots & 0 & \Theta_0 \end{bmatrix} \tag{36}$$

where $\Theta_k = t^{k\alpha}/\Gamma[1+k\alpha]$. Let us for now assume that the lower-right block-matrix of Eq. (35) vanishes asymptotically,

$$E_\alpha[J' t^\alpha] \to \mathbf{0}_{\tilde{n}\times\tilde{n}} \quad \text{as } t \to \infty. \tag{37}$$

We will first show that, under this condition, positions and velocities for this multiagent system reach consensus asymptotically. Once this is shown, we will investigate the conditions under which Eq. (37) is true.

Given the assumption Eq. (37), the transition matrix for our system approaches

$$\Phi_\alpha(t,0) = E_\alpha[A_c t^\alpha] \to V \begin{bmatrix} E_\alpha[J_0 t^\alpha] & \mathbf{0}_{n\times\tilde{n}} \\ \mathbf{0}_{\tilde{n}\times n} & \mathbf{0}_{\tilde{n}\times\tilde{n}} \end{bmatrix} W \quad \text{as } t \to \infty, \tag{38}$$

By inspection, the only eigenvectors which contribute to the pSTM asymptotically are those associated with the zero eigenvalues. Without loss of generality, we can choose these as

$$\begin{aligned} v_1 &= \begin{bmatrix} \mathbf{1}_N^T & \mathbf{0}_N^T & \mathbf{0}_N^T & \cdots & \mathbf{0}_N^T \end{bmatrix}^T \\ v_2 &= \begin{bmatrix} \mathbf{0}_N^T & \mathbf{1}_N^T & \mathbf{0}_N^T & \cdots & \mathbf{0}_N^T \end{bmatrix}^T \\ &\vdots \\ v_n &= \begin{bmatrix} \mathbf{0}_N^T & \mathbf{0}_N^T & \mathbf{0}_N^T & \cdots & \mathbf{1}_N^T \end{bmatrix}^T \end{aligned} \quad \text{and} \quad \begin{aligned} w_1 &= \begin{bmatrix} \boldsymbol{p}^T & \mathbf{0}_N^T & \mathbf{0}_N^T & \cdots & \mathbf{0}_N^T \end{bmatrix}^T \\ w_2 &= \begin{bmatrix} \mathbf{0}_N^T & \boldsymbol{p}^T & \mathbf{0}_N^T & \cdots & \mathbf{0}_N^T \end{bmatrix}^T \\ &\vdots \\ w_n &= \begin{bmatrix} \mathbf{0}_N^T & \mathbf{0}_N^T & \mathbf{0}_N^T & \cdots & \boldsymbol{p}^T \end{bmatrix}^T \end{aligned}$$

where $\mathbf{1}_N$ and $\mathbf{0}_N$ represent the $N \times 1$ vector of ones and zeros, respectively, and where $\boldsymbol{p}$ is the left-eigenvector of the graph Laplacian matrix L with eigenvalue 0, $\boldsymbol{p}^T L = 0$, normalized such that $\boldsymbol{p}^T \mathbf{1}_N = 1$. Note that the eigenvectors $\{v_k, w_k\}$, for $k = 2, 3, \ldots, n$, are *generalized* eigenvectors of v_1 and w_1.

Defining the submatrices $V_0 = [v_1 \ \cdots \ v_n]$ and $W_0 = [w_1 \ \cdots \ w_n]$ which contain the right- and left-eigenvectors associated with $\lambda = 0$, we write

$$V = \begin{bmatrix} V_0 & V_i \end{bmatrix} \quad \text{and} \quad W = \begin{bmatrix} W_0^T \\ W_i^T \end{bmatrix}. \tag{39}$$

Note that V_0 and W_0 have dimension $(nN \times n)$, while V_i and W_i (which contain the eigenvectors associated with the nonzero eigenvalues) have dimension $(nN \times n(N-1))$. In terms of these submatrices, Eq. (38) becomes

$$\Phi_\alpha(t,0) \to V_0 E_\alpha(J_0 t^\alpha) W_0^T = \begin{bmatrix} \Theta_0 \boldsymbol{P} & \Theta_1 \boldsymbol{P} & \cdots & \Theta_{n-1}\boldsymbol{P} \\ \mathbf{0} & \Theta_0 \boldsymbol{P} & \cdots & \Theta_{n-2}\boldsymbol{P} \\ \vdots & \ddots & \ddots & \vdots \\ \mathbf{0} & \cdots & \mathbf{0} & \Theta_0 \boldsymbol{P} \end{bmatrix} = E_\alpha[J_0 t^\alpha] \otimes \boldsymbol{P} \quad \text{as } t \to \infty, \tag{40}$$

where we have defined the $N \times N$ matrix $\boldsymbol{P} = \mathbf{1}_N \boldsymbol{p}^T$.

This transition matrix is used to find the asymptotic behavior of the N-agent system starting from some initial condition vector $\boldsymbol{X}_0$. Recall that in the global representation, the pseudostate system vector is defined as

$$\begin{aligned} \boldsymbol{X} &= \begin{bmatrix} \boldsymbol{z}^T & D^\alpha \boldsymbol{z}^T & D^{2\alpha}\boldsymbol{z}^T & \cdots & D^{(n-1)\alpha}\boldsymbol{z}^T \end{bmatrix}^T \\ &= [\boldsymbol{z}^T \ D^\alpha \boldsymbol{z}^T \ D^{2\alpha}\boldsymbol{z}^T \ \cdots \ \boldsymbol{x}^T \ D^\alpha \boldsymbol{x}^T \ \cdots \ \boldsymbol{v}^T \ D^\alpha \boldsymbol{v}^T \ \cdots \ D^{1-\alpha}\boldsymbol{v}^T]^T. \end{aligned}$$

From the definition of the Caputo derivative Eq. (14), if $\beta \notin \mathbb{N}$ then $D^\beta f(0) = 0$ for any function $f(x) \in C^k[0,T]$ given $T > 0$ and $k > \beta$ (see, *e.g.*, [25]). Additionally, since $\boldsymbol{z}$ represents the integrals of the positions of the agents from time 0 to t, $z_0 = \mathbf{0}$. Thus the only nonzero initial conditions are the initial positions and initial velocities of the N agents. These occupy the $\delta + 1$ and $2\delta + 1$ blocks of $\boldsymbol{X}$. Thus

$$\boldsymbol{X}_0 = [\underbrace{0 \ \cdots \ 0}_{\delta N \text{ zeros}} \ \boldsymbol{r}_0^T \ \underbrace{0 \ \cdots \ 0}_{(\delta-1)N \text{ zeros}} \ \boldsymbol{v}_0^T \ \underbrace{0 \ \cdots \ 0}_{(\delta-1)N \text{ zeros}}]^T$$

Using the asymptotic pSTM of Eq. (40) we find that the N-agent system asymptotically approaches

$$\boldsymbol{X}(t) = \Phi_\alpha(t,0)\boldsymbol{X}_0 = \begin{bmatrix} \boldsymbol{P}\tilde{\Theta}_\delta \boldsymbol{r}_0 + \boldsymbol{P}\tilde{\Theta}_{2\delta}\boldsymbol{v}_0 \\ \boldsymbol{P}\tilde{\Theta}_{\delta-1} \boldsymbol{r}_0 + \boldsymbol{P}\tilde{\Theta}_{2\delta-1}\boldsymbol{v}_0 \\ \vdots \\ \boldsymbol{0}_N \end{bmatrix} \quad \text{as } t \to \infty \tag{41}$$

where for brevity we have introduced the notation $\tilde{\Theta}_m$ which equals Θ_m for $m \geq 0$ and 0 for $m < 0$. The components of $\boldsymbol{X}(t)$ corresponding to position and velocity are given by

$$\begin{aligned} \boldsymbol{r}(t) &= \boldsymbol{P}\boldsymbol{r}_0 + \boldsymbol{P}\Theta_\delta \boldsymbol{v}_0 \\ \boldsymbol{v}(t) &= \boldsymbol{P}\boldsymbol{v}_0 \end{aligned} \qquad \text{as } t \to \infty \tag{42}$$

Since $\boldsymbol{P} = \boldsymbol{1}_N \boldsymbol{p}^T$ and $\Theta_\delta = t$, these asymptotic positions and velocities are

$$\begin{aligned} \boldsymbol{r}(t) &= \bar{r}\boldsymbol{1}_N + \bar{v}\boldsymbol{1}_N t \\ \boldsymbol{v}(t) &= \bar{v}\boldsymbol{1}_N \end{aligned} \qquad \text{as } t \to \infty \tag{43}$$

where $\bar{r} = \boldsymbol{p}^T\boldsymbol{r}_0$ represents a weighted average of the initial positions and $\bar{v} = \boldsymbol{p}^T\boldsymbol{v}_0$ represents a weighted average of initial velocities. The weighting is given by the components of $\boldsymbol{p}$, the left-eigenvector of L associated with $\mu_1 = 0$; this weighting therefore depends on the communication topology. For complete graphs, $\boldsymbol{p} = (1/N)\boldsymbol{1}_N$, so that $\bar{r}$ and $\bar{v}$ are simply the mean values of the initial positions and velocities, respectively. We therefore see that, as long as $E_\alpha[J' t^\alpha] \to \boldsymbol{0}$ as $t \to 0$ (as assumed in Eq. (38)), the multiagent system under PID$^\alpha$ consensus control comes to exact consensus in position and velocity asymptotically.

Returning now to the assumption of Eq. (37), let us first consider the case of simple non-zero eigenvalues, so that $J' = \mathrm{diag}(\lambda_{n+1}, \lambda_{n+2}, \ldots, \lambda_{nN})$. In this case,

$$E_\alpha[J' t^\alpha] = \mathrm{diag}(E_\alpha(\lambda_{n+1}t^\alpha),\, E_\alpha(\lambda_{n+1}t^\alpha),\, \ldots,\, E_\alpha(\lambda_{nN}t^\alpha)) \tag{44}$$

Since the ML function can be expanded asymptotically to give

$$E_\alpha(z) \to \frac{1}{\alpha}\exp\left(z^{1/\alpha}\right), \quad \text{as } |z| \to \infty$$

(see, *e.g.*, Theorem 3.1 of [22]), the diagonal elements of Eq. (44) approach

$$E_\alpha(\lambda_i t^\alpha) \to \frac{1}{\alpha}\exp\left(\lambda_i^{1/\alpha} t\right), \quad \text{as } t \to \infty \tag{45}$$

This vanishes asymptotically when the real part of $\lambda_i^{1/\alpha}$ is negative,

$$\mathrm{Re}\left\{\lambda_i^{1/\alpha}\right\} = \mathrm{Re}\left\{\left[|\lambda_i|\exp\left(i\arg\lambda_i\right)\right]^{1/\alpha}\right\} = \mathrm{Re}\left\{|\lambda_i|^{1/\alpha}\exp\left(i\,\frac{\arg\lambda_i}{\alpha}\right)\right\} = |\lambda_i|^{1/\alpha}\cos\left(\frac{\arg\lambda_i}{\alpha}\right) < 0,$$

giving the argument condition on the non-zero eigenvalues as

$$|\arg\lambda_i| > \alpha\frac{\pi}{2}, \qquad i = n+1, n+2, \ldots nN \tag{46}$$

This condition is a particular instance of Matignon's theorem [14].

If one or more of the non-zero eigenvalues are degenerate, then J' will then contain Jordan blocks corresponding to these degenerate eigenvalues. The matrix ML function of a Jordan block corresponding to a degenerate eigenvalue λ_d has elements built from $E_\alpha(\lambda_d t^\alpha)$ and its integer-order derivatives $\frac{d^m}{dt^m}E_\alpha(\lambda_d t^\alpha)$. From Eq. (45), if $E_\alpha(\lambda_d t^\alpha)$ vanishes asymptotically, so does its derivative. Therefore, $E_\alpha[J' t^\alpha]$ will vanish asymptotically if the non-zero eigenvalues satisfy Eq. (46), regardless of their geometric multiplicity.

Let us review what we have just shown in the preceding argument. We had assumed that the communication topology possessed a spanning tree, which implied that the graph Laplacian had a simple zero eigenvalue. We then showed that the closed-loop system of double-integrators under fractional PID$^\alpha$ consensus control — which was expressed in a pseudostate-space form having fractional order $\alpha = 1/\delta$ and dimension $nN = 3\delta N$ — then possessed exactly n zero-eigenvalues ($\lambda_i = 0$, $i = 1, \ldots, n$) of geometric multiplicity 1, and $n(N-1)$ potentially non-zero eigenvalues (λ_i, $i = n+1, \ldots, nN$). Under the condition that the latter set of eigenvalues were in fact non-zero and satisfied $|\arg \lambda_i| > \alpha\pi/2$, we then showed that the system asymptotically reaches consensus, with positions and velocities given by Eq. (42). Moreover, the speed at which consensus is reached is dependent on the vanishing of $E_\alpha[J' t^\alpha]$ in the lower-right block of the modal form of the pSTM, Eq.(35), and this block vanishes as

$$E_\alpha(-\rho t^\alpha). \tag{47}$$

We have therefore shown that, under the conditions stated above, the system is asymptotically stable in the Mittag-Leffler sense [24].

C. Stability Conditions on Gains — Fully-Connected Fractional-Order PID$^\alpha$

The PID$^\alpha$ consensus control protocol in commensurate form is given in Eq. (29), and repeated here for convenience:

$$u_i = \sum_{j=1}^{N} a_{ij} \left(k_I(\xi_j - \xi_i) + k_P D^{\delta\alpha}(\xi_j - \xi_i) + k_D D^{q\alpha}(\xi_j - \xi_i) \right),$$

with $\delta, q \in \mathbb{N}$ and with $\delta < q < 2\delta$. The pseudostate equations Eqs. (23) and (24) are therefore of dimension $nN = 3\delta N$, and K_n is an n-dimensional row matrix with k_I in the first position, k_P in the $(\delta + 1)$ position, k_D in the $(q + 1)$ position, and zeros elsewhere.

Let us now assume that the communication topology is fully connected, so that the eigenvalues of the graph Laplacian are given by Eq. (12). In this case, the characteristic equation of the closed-loop system is given by

$$0 = \lambda^n \det(\lambda I_n - A_n + N B_n K_n)^{N-1} \tag{48}$$
$$= \lambda^n (\lambda^n + N k_D \lambda^q + N k_P \lambda^\delta + N k_I)^{N-1} \tag{49}$$

so that the closed-loop system has n zero-eigenvalues, and n non-zero eigenvalues each with $(N-1)$-fold degeneracy. We can now find the regions in the $\{k_P, k_I, k_D\}$-space which correspond to systems which reach consensus asymptotically.

As we have shown, the closed-loop system will be asymptotically stable if $|\arg(\lambda_i)| > \frac{\alpha\pi}{2}$ for $i = n+1, \cdots, nN$. We can therefore trace the stability region in $\{k_I, k_D, k_P\}$-space by setting $\lambda = \rho e^{i\alpha\pi/2}$. The eigenvalues which must satisfy the stability requirement are found from

$$0 = \lambda^n + N k_D \lambda^q + N k_P \lambda^\delta + N k_I \tag{50}$$
$$= \rho^n \exp(i\frac{n\alpha\pi}{2}) + N k_D \rho^q \exp(i\frac{q\alpha\pi}{2}) + N k_P \rho^\delta \exp(i\frac{\delta\alpha\pi}{2}) + N k_I. \tag{51}$$

Since $n = 3\delta$ and $\delta = 1/\alpha$, this becomes

$$0 = \rho^n \exp(i\frac{3\pi}{2}) + N k_D \rho^q \exp(i\frac{q\alpha\pi}{2}) + N k_P \rho^\delta \exp(i\frac{\pi}{2}) + N k_I \tag{52}$$
$$= -i\,\rho^n + N k_D \rho^q \exp(i\frac{q\alpha\pi}{2}) + i\,N k_P \rho^\delta + N k_I. \tag{53}$$

Demanding that both real and imaginary parts must separately satisfy this equation gives

$$k_D \rho^q \cos\left(\frac{q\alpha\pi}{2}\right) + k_I = 0 \tag{54a}$$

$$N k_P \rho^\delta - \rho^n + N k_D \rho^q \sin\left(\frac{q\alpha\pi}{2}\right) = 0. \tag{54b}$$

Eliminating ρ using Eq. (54a) provides the following condition for an eigenvalue on the boundary of the stability region:

$$N k_P \left(\frac{-k_I}{k_D \cos\left(\frac{q\alpha\pi}{2}\right)} \right)^{\frac{\delta}{q}} - \left(\frac{-k_I}{k_D \cos\left(\frac{q\alpha\pi}{2}\right)} \right)^{\frac{3\delta}{q}} - N k_I \tan\left(\frac{q\alpha\pi}{2}\right) = 0. \tag{55}$$

In other words, this defines a hypersurface in $\{k_P, k_I, k_D\}$-space separating stable and unstable regions of parameter space. We therefore find that consensus will be reached asymptotically if

$$k_P > k_I \tan\left(\frac{q\alpha\pi}{2}\right) \left(\frac{-k_I}{k_D \cos\left(\frac{q\alpha\pi}{2}\right)} \right)^{-\frac{1}{q\alpha}} + \frac{1}{N} \left(\frac{-k_I}{k_D \cos\left(\frac{q\alpha\pi}{2}\right)} \right)^{\frac{2}{q\alpha}}. \tag{56}$$

We note that for standard integer-order PID control in this pseudostate form, $q = 2\delta = 2/\alpha$, and Eq. (56) reduces to

$$k_P > \frac{k_I}{N k_D} \tag{57}$$

which is exactly what we found in at the end of Section II.A.

To illustrate these stability conditions on the system gains, we will simulate a 3-agent fully-connected system with $\alpha_D = 0.5$. This corresponds to a system with commensurate fractional order $\alpha = 0.5$ and thus $n = 3/\alpha = 6$ pseudostate components per agent. As the system is fully connected, the closed-loop system matrix A_c has 6 zero-eigenvalues and 6 non-zero eigenvalues each with degeneracy 2 (*i.e.*, a total of 12 nonzero eigenvalues). If we choose $k_I = 2$ and $k_D = 1$, we find from Eq. (56) that the system should be asymptotically stable if $k_P > 1/3$. In Fig. 3 we show three choices of k_P which correspond to asymptotically stable behavior ($k_P = 1$), marginally stable behavior ($k_P = 1/3$), and unstable behavior ($k_P = 0.1$). We also show the eigenvalues of the system matrix A_c in all three cases. We see that stable behavior indeed corresponds the case $k_P = 1$ where the non-zero eigenvalues of A_c satisfy $|\arg \lambda_i| > \alpha\pi/2$, and unstable behavior corresponds to $k_P = 0.1$ where this eigenvalue condition is violated.

V. Numerical Simulations

In this section we will report numerical simulation results of multiagent second-order systems under fractional control protocols of the form in Eq. (29). We first describe how these numerical results are generated using the fractional Chebyshev collocation method. We will then illustrate how the extra degree of freedom available from the fractional order α_D can generally lead to better controller performance by simulating the evolution of three benchmark systems and varying α_D. Lastly, we will show that the optimal choice of gains using the fractional PID$^\alpha$ controller outperforms the optimal choice of gains using the integer-order controller for the fully connected system, providing a concrete illustration of the advantages of fractional order controllers.

A. Fractional Chebyshev Collocation Method

Since we will be surveying over large swaths of parameter space in order to compare integer- and fractional-order controllers, we require an efficient method of numerical solution for fractional differential equations. We will utilize the fractional Chebychev collocation (FCC) method developed in [28–30], outlined as follows.

Consider the fractional-order system

$$D^\alpha[\mathbf{x}(t)] = A\,\mathbf{x}(t) + B\mathbf{u}(t), \quad \mathbf{x}_0 = [x_1(0) \;\; \cdots \;\; x_n(0)]^T \tag{58}$$

where $\mathbf{x}(t) = [x_1(t), \cdots, x_n(t)]^T$, $\mathbf{u}(t) \in \mathbb{R}^m$, A and B are $n \times n$ and $n \times m$ matrices, respectively, $0 < \alpha \leq 1$, and $D^\alpha[\mathbf{x}(t)]$ represent the n-dimensional fractional derivatives of the state and are defined as

$$D_t^\alpha[\mathbf{x}(t)] \equiv \left[D_t^\alpha[x_1(t)] \quad D_t^\alpha[x_2(t)] \quad \cdots \quad D_t^\alpha[x_n(t)] \right]^T \tag{59}$$

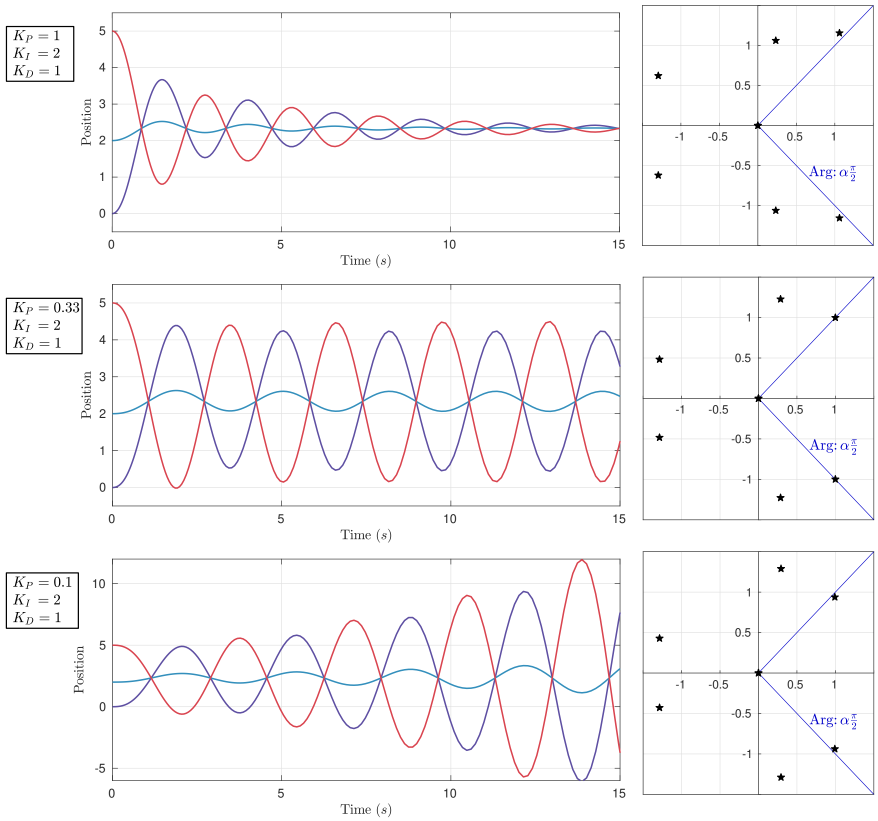

Fig. 3 Illustrating the stability conditions on gains for a fully-connected system under fractional PID$^\alpha$ control. For this 3-agent system, we have taken derivative order $\alpha_D = 0.5$ and chosen $k_I = 2$ and $K_D = 1$. Using Eq. (56), we find that the system will be stable for $k_P > 0.33$. We show choices of k_P at, above, and below this stability limit. In the right panels we show the location of the eigenvalues of the system matrix A_c corresponding to these choices of k_P. These plots agree with our result that the system is asymptotically stable if the non-zero eigenvalues of A_C satisfy $|\arg \lambda_i| > \alpha\frac{\pi}{2}$.

We want to discretize the solution of the system (58) at the Chebyshev-Gauss-Lobatto points $\mathbf{t}_d = [t_0, t_1, \ldots, t_{N-1} = \tau]^T$ as the extrema of the Chebyshev polynomial $T_N(x)$ where

$$t_k = \cos\left(\frac{k\pi}{N-1}\right), \quad k = 0, 1, \ldots, N-1, \tag{60}$$

and the n^{th}-degree Chebyshev polynomial of the first kind $T_n(t)$ is defined by the recurrence relation

$$T_n(t) = 2tT_{n-1}(t) - T_{n-2}(t), \quad n = 2, 3, \cdots, \tag{61}$$

where $T_0(t) = 1$ and $T_1(t) = t$.

For this purpose, we use the FCC framework [28]: Let the discretized matrix of any $n \times m$ matrix P at the collocation points $\mathbf{t}_d$ be defined as

$$\bar{P}_d := P \otimes \bar{I}_N, \tag{62}$$

where $\bar{I}_N$ is defined as a modified $N \times N$ identity matrix whose first row is replaced by a zero row of the same size.

Similarly, for an $n \times 1$ constant vector $\mathbf{v} = [v_1, v_2, \cdots, v_n]^T$ and an $n \times 1$ vector function $\mathbf{u}(t) = [u_1(t), u_2(t), \cdots, u_n(t)]^T$, $\{\mathbf{v}\}_d$ and $[\mathbf{u}]_d$ are defined as

$$\{\mathbf{v}\}_d : \;=\; \mathbf{v} \otimes \bar{\mathbf{1}}, \tag{63a}$$
$$[\mathbf{u}]_d : \;=\; [u_1(\mathbf{t}_d^T) \;\; u_2(\mathbf{t}_d^T) \;\; \cdots \;\; u_n(\mathbf{t}_d^T)]^T, \tag{63b}$$

where $\bar{\mathbf{1}}$ is an $N \times 1$ column vector whose elements are all zeros expect the last element which is one.

The left-sided fractional Chebyshev differentiation matrix denoted by $\mathbb{D}^{\alpha}_{N+1}$ is a linear map that maps the discretized function $\mathbf{x}_d$ at the Chebyshev-Gauss-Lobatto points $\mathbf{t}_d = [t_0 = a, t_1, \cdots, t_{N-1}, t_N = b]$ onto the discretized value of $D^{\alpha}[x(t)]$ at those points

$$\mathbb{D}^{\alpha}_{N+1}\mathbf{x}_d = \Big[[D^{\alpha}[x(t)]]_{t=a}, \; \big[D^{\alpha}_t[x(t)]\big]_{t=t_1}, \; \cdots, \; [D^{\alpha}[x(t)]]_{t=b} \Big].$$

The left-sided fractional Chebyshev differentiation matrix has been obtained in [29, 30].

Let $\mathbf{x}^T_{d i,\tau}$, $i = 1, 2, \cdots, n$, denote discretized $x_i(t)$ at collocation points $\mathbf{t}_d$ such that $\mathbf{x}_{d,\tau} = [\mathbf{x}^T_{d 1,\tau}, \cdots, \mathbf{x}^T_{d n,\tau}]^T$. Then, the discretized solution of the system Eq. (58) is obtained by a discretized state transition matrix $T_{d,\tau}$ as [28]

$$\mathbf{x}_{d,\tau} = T_{d,\tau} \left(\{\mathbf{x}_0\}_d + \bar{B}_d \, [\mathbf{u}]_d \right), \quad t_0 \le t \le \tau, \tag{64}$$

where

$$T_{d,\tau} \;\; = \;\; \left(I_n \otimes \bar{I}_N \; \mathrm{D}^{\alpha}_N - \bar{A}_d \right)^{-1},$$

where $\bar{A}_d$ and $\bar{B}_d$ are the discretized matrices of A and B obtained by Eq. (62), $\{\mathbf{x}_0\}_d$ is the discretized vector of $\mathbf{x}_0$ obtained by Eq. (63a), and $[\mathbf{u}]_d$ is the discretized vector of $\mathbf{u}(t)$ obtained by Eq. (63b).

B. Performance Comparisons Between Fractional and Integer-Order Controllers

We will now report the results of a survey over a subset of the parameter space which will illustrate the advantages of fractional PID$^{\alpha}$ controllers. The communication topology of three benchmark multiagent systems we will consider here are illustrated below.

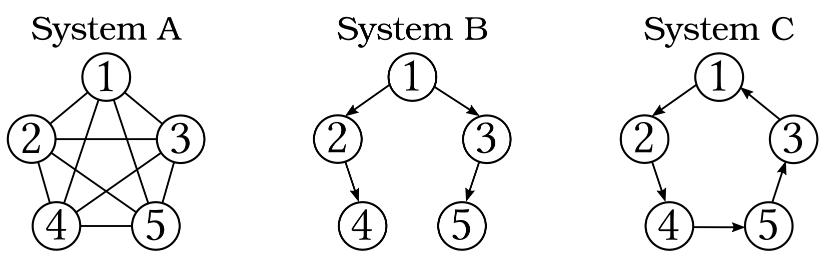

System A represents a fully connected communication topology, System B represents a leader-follower type communication topology, and System C represents a cyclical communication topology. The graph Laplacian matrices for these three systems are given by

$$L_A = \begin{bmatrix} 4 & -1 & -1 & -1 & -1 \\ -1 & 4 & -1 & -1 & -1 \\ -1 & -1 & 4 & -1 & -1 \\ -1 & -1 & -1 & 4 & -1 \\ -1 & -1 & -1 & -1 & 4 \end{bmatrix}, \quad L_B = \begin{bmatrix} 0 & 0 & 0 & 0 & 0 \\ -1 & 1 & 0 & 0 & 0 \\ -1 & 0 & 1 & 0 & 0 \\ 0 & -1 & 0 & 1 & 0 \\ 0 & 0 & -1 & 0 & 1 \end{bmatrix}, \quad L_C = \begin{bmatrix} 1 & 0 & -1 & 0 & 0 \\ -1 & 1 & 0 & 0 & 0 \\ 0 & 0 & 1 & 0 & -1 \\ 0 & -1 & 0 & 1 & 0 \\ 0 & 0 & 0 & -1 & 1 \end{bmatrix}. \tag{65}$$

Note that eigenvalues for L_A are given as in Eq. (12), nonzero eigenvalues of L_B are equal to unity, and nonzero eigenvalues for L_C are complex.

Each of the five agents are assumed to have a mass of 1 kg, are initialized at rest at the positions $\boldsymbol{r}_0 = [1 \;\; 2 \;\; 4 \;\; 7 \;\; 9]^T$ (meters), and are controlled by the protocol of Eq. (29). We will set $k_P = 1$ universally, and survey over the remaining free parameters of the controller, $\{k_I, \; k_D, \; \alpha_D\}$. The consensus values in position $\bar{r}$ are found from the left-eigenvector $\boldsymbol{p}$ of the respective Laplacian matrices corresponding to the zero eigenvalue, $\bar{r} = \boldsymbol{p}^T \boldsymbol{r}_0$, as discussed below Eq. (43). For these three systems the consensus values are $\bar{r}_A = 4.6$ m, $\bar{r}_B = 1.0$ m, $\bar{r}_C = 4.6$ m. All numerical results were generated using the FCC method outlined above and implemented in Matlab; results were selectively cross-checked against results obtained from the PECE method [31], showing good agreement.

We first survey over $\alpha_D = [0, 1]$ given $k_I = 1$ and k_D chosen such that the integer-order PID control gives stable behavior. For each point in this survey we compute settling time t_s and overshoot for the system. These performance specifications are determined as follows:

- **Settling time:** First we determine the average distance of the initial positions from the consensus value. We then compute the time it takes for each agent to fall and remain within 15% of this average initial distance. The agent which takes the longest to reach and remain within this window defines the settling time for the system.
- **Overshoot:** We first determine, when applicable, the time at which each agent crosses the consensus value. From this time forward, we determine the largest difference between the agent's position and the consensus value. Normalizing this difference to the initial difference between the position and the consensus value gives the percent overshoot for that agent. For over-damped systems for which the agent never crosses the consensus value, we set the overshoot for this agent to zero. The collective overshoot of the entire system is defined as the largest overshoot among all N agents.

The results of this survey are shown in Fig.4. We plot both settling time and overshoot as a function of fractional order α_D for each of the three systems. We also plot the trajectories of the five agents using the integer-order controller (red) and the fractional-order controller (blue), where in the latter case we have chosen an approximately optimal value from the survey over α_D.

In all three cases we see that performance — in terms of both settling time *and* overshoot — is optimized by taking the derivative to non-integer order. For System A the optimal fractional order is found to be $\alpha_D \approx 0.55$, giving a reduction in settling time of 41% (from 5.76 s to 3.35 s) and reduction in overshoot by 75% (from 42% to 11%). For System B the optimal fractional order is taken to be $\alpha_D \approx 0.6$ (though the optimal value depends on which performance specification we are interested in), giving a reduction in settling time of 75% (from $\approx$ 30 s to 7.17 s) and reduction in overshoot by 54% (from 83% to 38%). We notice that this system generally responds slower than the fully connected system, which is intuitively expected due to the fact that there are fewer edges in the communication topology. Finally, for System C the optimal fractional order is found to be $\alpha_D \approx 0.75$, giving a reduction in settling time of 50% (from 20.0 s to 10.1 s) and reduction in overshoot by 46% (from 61% to 33%).

For a more robust comparison between the fractional PID$^{\alpha}$ and integer-order PID controller, we perform a survey over three of the four free parameters in our controller design, α_D, k_I, and k_D, keeping proportional gain constant at $k_P = 1$. We have simulated System A over a $(20 \times 20 \times 20)$-dimensional grid in $\{k_D,\ k_I,\ \alpha_D\}$ parameter space, using 20 different values of α_D evenly spaced between 0 and 1. We can observe the effects of using fractional derivative control by plotting settling time for "slices" of $\{k_I,\ k_D\}$ parameter space along different values of fractional order α_D. The slice at $\alpha_D = 1$ represents the integer-order PID controller, and we find the optimal settling time to be $t_s = 1.067$ s at $k_I = 0.05$ and $k_D = 0.60$. Allowing α_D to vary, we find that we can reduce settling time for this system to a global minimum of $t_s = 0.862$ s by taking $\alpha_D = 0.75$, $k_I = 0.25$, and $k_D = 0.60$. This corresponds to a 19% reduction in settling time, which is a substantial improvement. We show the two relevant slices of parameter space as contour plots in Fig. 5.

We can also compare the fractional- and integer-order controllers with respect to combined performance specifications. One particularly useful combined measure for multivehicle control is the simultaneous optimization of settling time and integrated control effort (which in real-world systems would correspond to fuel cost). A straightforward measure of this combined performance is to compute the geometric mean of the two quantities,

$$J = \sqrt{U \cdot t_s} \tag{66}$$

where integrated control effort U is computed as

$$U = \sum_{i=1}^{N} \int_0^T |u_i| dt.$$

This cost function is computed at all points in our survey grid; for our simulations we have taken $T = 30$ s. The relevant slices of parameter space for this survey are shown in Fig. 6.

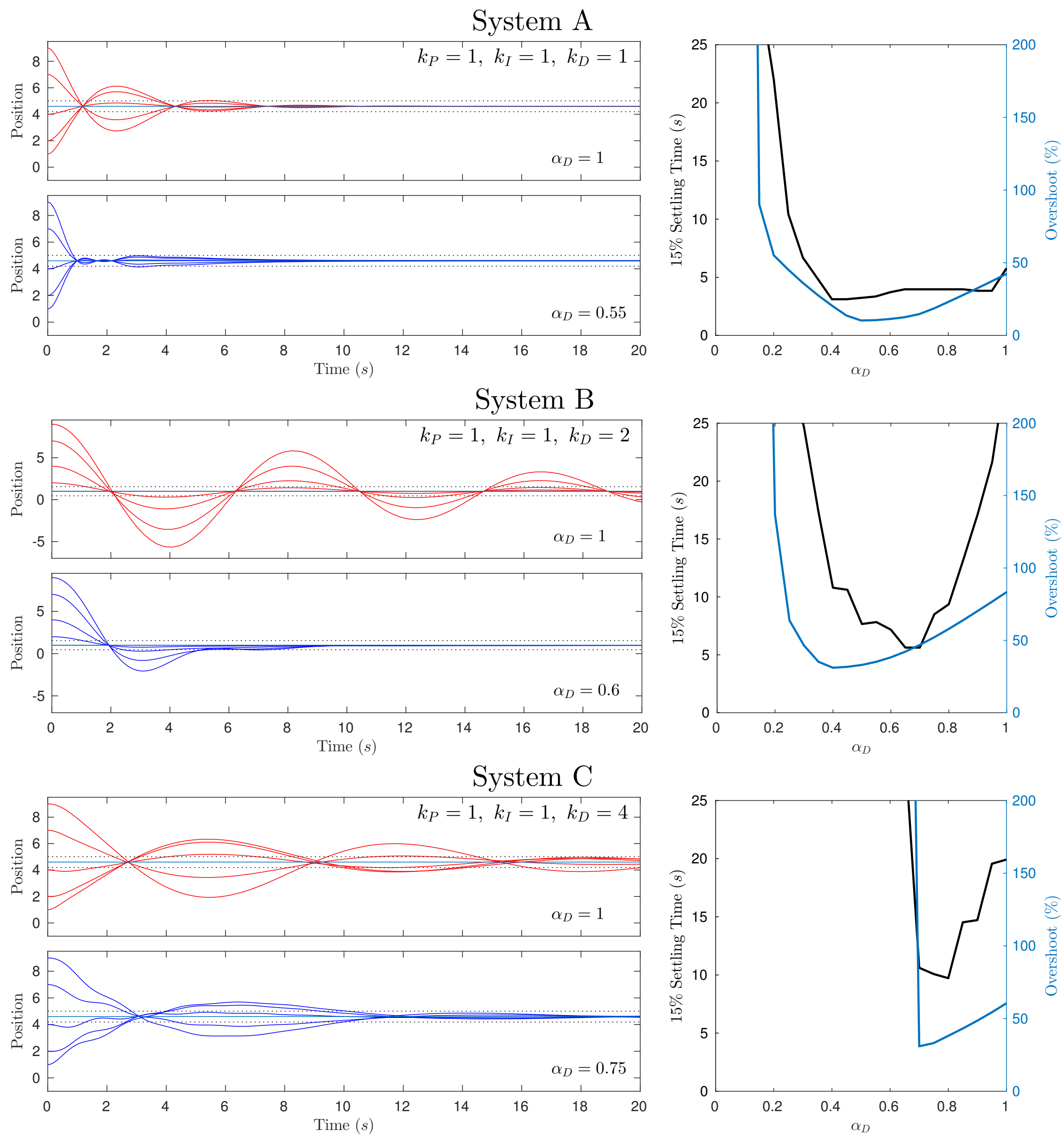

Fig. 4 Comparisons between integer- and fractional order consensus for the three systems in Eq. (65)**. In the left panels we show the system responce from an integer order PID controller in red and the response from a fractional order PID$^{\alpha}$ controller (using the approximately optimal choice of α_D) in blue. In the right panels we show the settling time and overshoot for the system as a function of fractional derivative order α_D.**

For the integer-order controller, we find the optimal value to be $J = 5.83$ (having units of $\sqrt{\text{m}}$) at $k_I = 0.05$ and $k_D = 0.70$. The global optimal value of J is again found for non-integer order α_D. We find this global optimum to be $J = 5.78$, at $\alpha = 0.90$, $k_I = 0.20$ and $k_D = 0.70$. This corresponds to a slight reduction of 1%. Although the reduction is essentially negligible in this case, we take this as a proof of principle and note that cost function in Eq. (66) was constructed in a somewhat ad-hoc manner in order to eliminate the differences in scale between settling time and integrated cost.

By inspection of the left-panels of both Figs. 4 and 6 (where fractional derivative control is used) we find that performance is sub-optimal when integer gain k_I is taken to zero. As alluded to in Section II.B, the increase in settling time that is observed as $k_I \to 0$ is caused by the "creeping" behavior illustrated in Fig. 2. Hence we see that integral

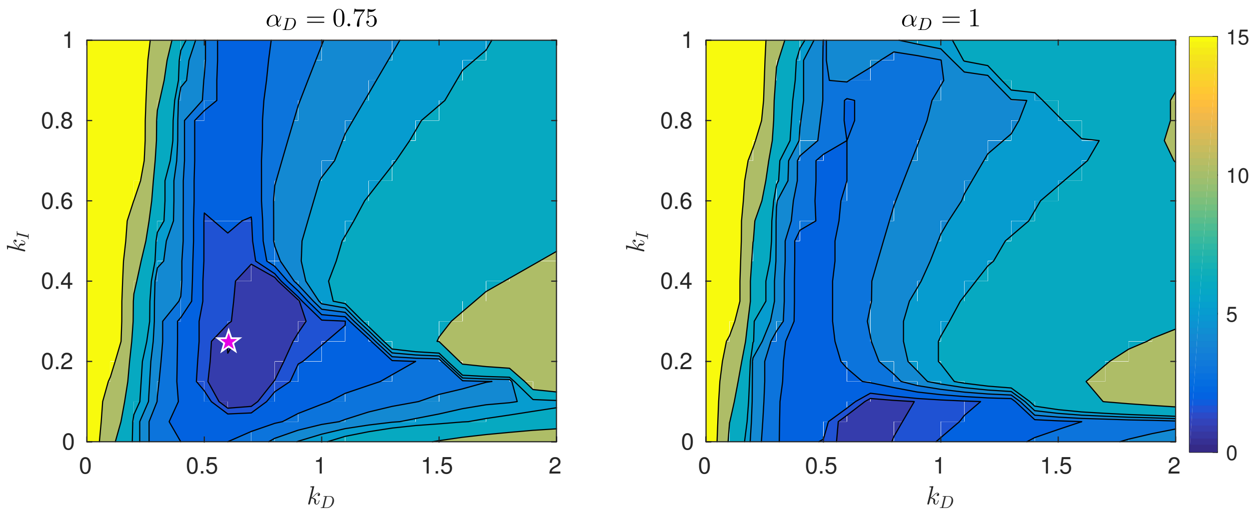

Fig. 5 Contours of settling time as a function of k_I and k_D for System A and taking $k_P = 1$. At left we show the contours for the fractional PID$^\alpha$, taking $\alpha_D = 0.75$, and at right we show the same results using integer order controller. After surveying over α_D, we have found that the minimum settling time of $t_s = 0.862$ s is acheived with a fractional controller using $\alpha_D = 0.75$, $k_D = 0.6$, and $k_I = 0.25$; this point is marked with a purple star. The minimum settling time for the integer-order controller is $t_s = 1.067$ s.

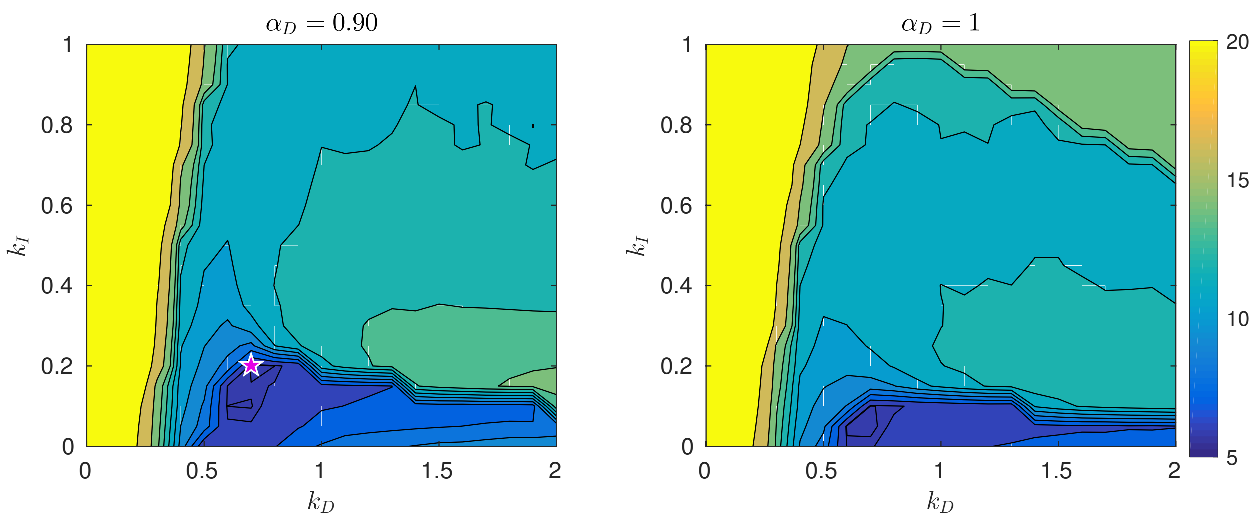

Fig. 6 Same as Fig. 5, but showing contours of the geometric mean of settling time and integrated control effort. In this case we find the optimal value to be 5.78 using the fractional controller with $\alpha_D = 0.90$, $k_D = 0.7$, $k_I = 0.2$. The minimum value using the integer-order controller is 5.83.

control has the effect of mitigating this creeping behavior and bringing the system to consensus more rapidly. On the other hand, for integer-order control (right panels of Figs. 4 and 6) we find that optimal behavior (for these performance specifications) is achieved for $k_I \approx 0$. Nevertheless, integral control can have utility in integer-order controllers in cases where one needs more freedom in shaping the system's response, or when mitigation of steady-state error is required.

The above simulation results provide a concrete demonstration of the benefits of using fractional PID$^\alpha$ consensus controllers for second-order multiagent systems. We note here that similar simulations have been performed for non-zero initial velocities, and similar results were obtained.

VI. Conclusions

The automated control of multivehicle systems is a topic which has gained a considerable amount of interest in recent years. In this work, we have presented a number of novel results relevant to this field. As our primary contribution, we have formulated a fractional PID$^\alpha$-type consensus controller, generalizing the standard PD-type controllers typically utilized for second-order multiagent systems. This controller incorporates a derivative term whose order can be tuned between 0 and 1; this fractional derivative term thus serves as an extra "knob" that one can tune, allowing more freedom in how one can shape the response of the system. It was proved that, under the condition that all non-zero eigenvalues of the pseudostate system matrix satisfy $|\arg \lambda_i| > \alpha\pi/2$, the controller drives the multiagent system to consensus asymptotically. This condition on the non-zero eigenvalues was then related to the free parameters of the controller, $\{\alpha_D,\ k_P,\ k_I,\ k_D\}$, and stability conditions on the gains were obtained for both integer-order and, in the case of fully connected topologies, fractional-order PID consensus controllers. As a corollary to this latter result, we find that a fully-connected second-order multiagent system under standard, integer-order PID control will be stable if $k_I < N k_P k_D$, where N is the number of agents in the system.

We have also demonstrated the efficacy of the PID$^\alpha$ consensus controller numerically by simulating the behavior of several benchmark 5-agent systems. For a 5-agent system with fully-connected communication topology, we have shown that the fractional PID$^\alpha$ outperforms the optimal integer-order PID controller (in terms of a few important performance specifications) by surveying over the controller parameter space.

References

[1] Ren, W., Beard, R. W., and Atkins, E. M., "Information Consensus in Multivehicle Cooperative Control," *IEEE Control Systems*, Vol. 27, No. 2, 2007, pp. 71–82. doi: 10.1109/MCS.2007.338264

[2] Fax, J. A., and Murray, R. M., "Information Flow and Cooperative Control of Vehicle Formations," *Transactions on Automatic Control*, Vol. 49, No. 9, 2004, pp. 1465–1476. doi: 10.1109/TAC.2004.834433

[3] Lewis, F. L., Zhang, H., Hengster-Movric, K., and Das, A., *Cooperative Control of Multi-Agent Systems*, Springer, New York, 2014. doi: 10.1007/978-1-4471-5574-4

[4] Ren, W., and Atkins, E. M., "Distributed Multi-vehicle Coordinated Control via Local Information Exchange", *International Journal of Robust and Nonlinear Control*, Vol. 17, No. 10–11, 2007, pp. 1002–1033. doi:10.1002/rnc.1147

[5] Ren, W., "On Consensus Algorithms for Double-Integrator Dynamics", *Transactions on Automatic Control*, Vol. 53, No. 6, July 2008, pp. 1503–1509. doi: 10.1109/TAC.2008.924961

[6] Yucelen, T., and Johnson, E. N., "Control of Multivehicle Systems in the Presence of Uncertain Dynamics," *International Journal of Control*, Vol. 86, No. 9, 2013, pp. 1540–1553. doi: 10.1080/00207179.2013.790077

[7] Wheeler, N., "Construction and Physical Application of the Fractional Calculus," Reed College e-print (1997).

[8] Chen, Y., Petras, I., and Xue, D., "Fractional Order Control – A Tutorial," *2009 American Control Conference*, ACC, St. Louis, MO, 2009, pp. 1397–1411. doi: 10.1109/ACC.2009.5160719

[9] Oldham, K. B., and Spanier, J., *The Fractional Calculus; Theory and Applications of Differentiation and Integration to Arbitrary Order*, Academic Press, San Diego, 1974.

[10] Gutierrez, R. E., Rosario, J. M., and Machado, J. T., "Fractional Order Calculus: Basic Concepts and Engineering Applications," *Mathematical Problems in Engineering*, 2010, Article ID: 375858. doi:10.1155/2010/375858

[11] Bagley, R. L., and Calico, R. A., "Fractional Order State Equations for the Control of Viscoelastically Damped Structures", *Journal of Guidance, Control, and Dynamics*, Vol. 14, No. 2, 1991, pp. 304–311.

[12] Oustaloup, A., *La commande CRONE: Commande Robuste d'Ordre Non Entier*, Herme's, Paris, 1991.

[13] Podlubny, I., "Fractional-order systems and PI$^\lambda$D$^\mu$-controllers," *IEEE Transactions on Automatic Control*, Vol. 44, No. 1, 1999, pp. 208–214. doi: 10.1109/9.739144

[14] Matignon, D., "Stability Results for Fractional Differential Equations with Applications to Control Processing," *Computational Engineering in Systems Applications*, Lille, France, July 1996, pp. 963–968.

[15] Xue, D., Zhao, C., and Chen, Y., "Fractional order PID control of a DC-motor with elastic shaft: a case study," *Proceedings of the American Control Conference*, Minneapolis, MN, 2006. doi: 10.1109/ACC.2006.1657207

[16] Butcher, E. A., Nazari, M., Dabiri, A., and Sanyal, A. K., "Fractional PID Control of Spacecraft Attitude Dynamics using Rotation Matrices," *Proceedings of the International Astronautical Congress*, IAC, Guadalajara, 2016.

[17] Song, C., and Cao, J., "Consensus of fractional-order linear systems," *9th Asian Control Conference*, ASCC, Istanbul, 2013, pp. 1–4. doi: 10.1109/ASCC.2013.6606402

[18] Yucelen, T., and Egerstedt, M., "Control of Multiagent Systems under Persistent Disturbances," *2012 American Control Conference*, ACC, Montreal, QC, 2012, pp. 5264–5269. doi: 10.1109/ACC.2012.6314791

[19] Miller, K. S., and Ross, B., *An Introduction to the Fractional Calculus and Fractional Differential Equations*, John Wiley & Sons, Inc. New York, 1997.

[20] Podlubny, I., *Fractional Differential Equations*, Academic Press, San Diego, 1999.

[21] Monje, C. A., Chen, Y. Q., Vinagre, B. M., Xue, D., and Feliu, V., *Fractional-order Systems and Controls: Fundamentals and Applications*, Springer, New York, 2010. doi: 10.1007/978-1-84996-335-0

[22] Valerio, D., and da Costa, J. S., *An Introduction to Fractional Control*, The Institution of Engineering and Technology, London, 2013. doi: 10.1049/PBCE091E

[23] Caponetto, R., Dongola, G., Fortuna, L., and Petras, I., *Fractional Order Systems: Modeling and Control Applications*, World Scientific, New Jersey, 2010.

[24] Li, Y., Chen, Y., and Podlubny, I., "Stability of Fractional-order Nonlinear Dynamic Systems: Lyapunov Direct Method and Generalized Mittag–Leffler Stability," *Computers and Mathematics with Applications*, Vol. 59, 2010, pp. 1810–1821. doi:10.1016/j.camwa.2009.08.019

[25] Diethelm, K., and Ford, N. J., "Numerical Solution of the Bagley-Torvik Equation," *BIT Numerical Mathematics*, Vol. 42, No. 3, 2002, pp. 490–507.

[26] Dabiri, A., and Butcher, E. A., "Design of Optimal Fractional Luenberger Observers for Linear Fractional-Order Systems," *International Design Engineering Technical Conferences and Computers and Information in Engineering Conference*, ASME, Cleveland, OH, 2017. doi: 10.1115/DETC2017-68328

[27] N'doye, I., Zasadzinski, M., Darouach, M., and Radhy, N.-E., "Observer-based control for fractional-order continuous-time systems," *Proccedings on the Joint* 48^{th} *IEEE Conference on Decision and Control*, IEEE, Shanghai, 2009, pp. 1932–1937.

[28] Dabiri, A., and Butcher, E. A., "Numerical Solution of Multi-order Fractional Differential Equations with Multiple Delays via Spectral Collocation methods," *Applied Mathematical Modeling*, Vol. 56, 2018, pp. 424–448.

[29] Dabiri, A., and Butcher, E. A., "Efficient Modified Chebyshev differentiation Matrices for Fractional Differential Equations," *Communications in Nonlinear Science and Numerical Simulation*, Vol. 50, 2017, pp. 584–310.

[30] Dabiri, A., and Butcher, E. A., "Stable Fractional Chebyshev Differentiation Matrix for Numerical Solution of Fractional Differential Equations," *Nonlinear Dynamics*, Vol. 90, No. 1, pp. 185–201, 2017.

[31] Garrappa, R., "On Linear Stability of Predictor-corrector Algorithms for Fractional Differential Equations," *International Journal of Computer Mathematics*, Vol. 87, No. 10, 2010, pp. 2281–2290.